Effect of transfer agent, temperature and initial monomer concentration on branching in poly(acrylic acid): A study by 13 C NMR spectroscopy and capillary electrophoresis

Jean-Baptiste Lena, Alexander K Goroncy, Joel J Thevarajah, Alison R Maniego, Gregory T Russell, Patrice Castignolles, Marianne Gaborieau

Effect of transfer agent, temperature and initial monomer concentration on branching in poly(acrylic acid): a study by ^{13}C NMR spectroscopy and capillary electrophoresis

Jean-Baptiste Lena[a,b,c], Alexander K. Goroncy[a], Joel J. Thevarajah[b,c], Alison R. Maniego[b,c], Gregory T. Russell[a,*], Patrice Castignolles [b,*], Marianne Gaborieau[b,c]

[a] *Department of Chemistry, University of Canterbury, Private Bag 4800, Christchurch, New Zealand*
[b] *Western Sydney University, Australian Centre for Research on Separation Science (ACROSS) , School of Science and Health, Locked Bag 1797, Penrith NSW 2751, Australia*
[c] *Western Sydney University, Molecular Medicine Research Group, School of Science and Health, Locked Bag 1797, Penrith NSW 2751, Australia*

* Corresponding authors. Tel. +64 3 3642458 (GTR), +61 2 9685 9970 (PC)
E-mail addresses: jean-baptiste.lena@pg.canterbury.ac.nz (J.-B. Lena), greg.russell@canterbury.ac.nz (G.T. Russell), p.castignolles@westernsydney.edu.au (P. Castignolles), m.gaborieau@westernsydney.edu.au (M. Gaborieau)

ABSTRACT

Branching has been investigated in poly(acrylic acid) synthesized by conventional radical polymerization with and without chain transfer agent (CTA) at different temperatures and initial monomer concentrations. The average number of branches per monomer unit (i.e. degree of branching) was quantified by solution-state ^{13}C NMR spectroscopy. The heterogeneity of branching (dispersity of the electrophoretic mobility distributions) was measured by capillary electrophoresis in the critical conditions (CE-CC). The degree of branching (*DB*) increases with the reaction temperature due to a rise in the frequency of reactions leading to branches, while the heterogeneity of branching remains steady. *DB* is lower in polymer synthesized with CTA. This decrease is due to either the CTA quenching the mid-chain radicals or a reduction of the rate of chain transfer to polymer relative to (chain-end) propagation. No influence of initial monomer concentration on *DB* and on the heterogeneity of branching was observed.

Keywords:
Capillary Electrophoresis
Solution-State NMR spectroscopy
Branching

1. Introduction

Poly(acrylic acid) (PAA) is a water-soluble polymer with a wide range of applications, for example as superabsorbent [1], water purification aid [2], drug carrier [3, 4] and scale control agent [5]. Even if it is not always acknowledged, PAA is branched when produced by radical polymerization [6-8]. The branching strongly influences the properties of the polymer. Short branches influence physical properties such as melting point and glass transition temperature whilst long branches affect rheology [9]. One consequence of the branching can be inaccurate determination of the propagation rate coefficient, k_p, by pulse-laser polymerization (PLP) coupled with size exclusion chromatography (SEC)[10]. Long-chain branching (LCB) was detected even at low conversion and it was shown that it can decrease the accuracy of the molar mass determined by SEC, and hence the k_p obtained is less accurate (up to 100 % error) [11]. The molar masses of PAAs determined by SEC showed low accuracy [12] potentially due to long-chain branching. In terms of kinetics, LCB results from intermolecular chain transfer to polymer (or random intramolecular transfer to polymer) and short-chain branching (SCB) results from intramolecular transfer to polymer such as backbiting [13]. In both cases, the secondary propagating radical (SPR) is transformed into a mid-chain radical (MCR) (see Figure S1). The MCR can propagate but with a rate coefficient, k_p^{tert}, much lower than k_p. Intramolecular transfer to polymer thus influences the polymerization rate and can lead to inaccurate k_p values determined by PLP if not at low enough polymerization temperature [10, 14, 15] or high enough pulse frequency[16]. Studying the branching in PAA obtained by radical polymerization thus gives important information regarding its kinetics.

The only method to determine the average degree of branching (*DB)* in PAA is quantitative ^{13}C NMR spectroscopy. *DB* is expressed in percents of monomer units and is determined from the integration of the signal of the quaternary carbons (C_q) characteristic of a branched polymer and of a signal of a carbon whose characteristics remain unchanged in the branched and unbranched monomer units. This method has been utilized several times in order to determine *DB* in PAA [6, 8, 18] and poly(alkyl acrylate)s [17, 19-24]. Both resolution and sensitivity are required for reliable quantification of *DB*. Various NMR methods (solution-state, solid-state and melt-state) were previously compared for poly(n-alkyl acrylate)s [20]. However, optimal analyses were by melt-state NMR spectroscopy obtained at 150 °C above the

glass transition temperature (T_g) [20]. As the T_g of PAA is relatively high (between 90 and 150 °C) and PAAs degrade between 250 and 400 °C [25], the branching in PAA was determined in this work by solution-state NMR spectroscopy.

In 2010, Gaborieau *et al.* studied the influence of the polymerization temperature and presence of 1-octanethiol on the branching in poly(*n*-butyl acrylate) [17]. They confirmed that *DB* increases with temperature and showed that *DB* is considerably reduced when 1-octanethiol (as a chain transfer agent, CTA) is present amongst the reactants. The temperature increases the frequency of the reaction which leads to formation of MCRs. MCR species can then take 4 different pathways: propagation of the tertiary radical, which leads to a branched polymer; β-scission, which does not lead to a branched polymer (at least not directly); a "patching" reaction, in which a hydrogen radical is transferred from the 1-octanethiol to an MCR; and radical-radical termination (Figure S1). *DB* is measurably reduced when 1-octanethiol is present; this has been attributed to "patching". Ballard *et al.* [21] showed that there is another possible explanation for the decrease of *DB*. The presence of CTA may reduce the number of backbiting events in comparison to the number of propagation events as the macroradical polymerizes for a shorter time when the reaction is carried out with a CTA and the chains formed after only a few propagation events are too short to undergo backbiting.

The development of electrospray-ionization mass spectrometry (ESI-MS) has been useful to determine the product spectrum of a polymer sample and its changes within the chain length distribution [26]. A higher level of polymer characterization has become available, in that polymer chains can be 'visualized' precisely according to their end groups and chain length. The influence of temperature and of chain-transfer-agent (CTA) concentration on the structure of poly(*n*-alkyl acrylate)s has been studied by ESI-MS [27, 28]. The amount of β-scission increased with temperature and decreased with CTA concentration. However, linear and branched species cannot be distinguished by ESI-MS, which gives molar masses but no information related to branching. It is however challenging to obtain consistent ionization of different macromolecules within a sample. Different end-groups [29] or molar masses [30] can for example affect the ionization efficiency. This can thus limit the accuracy of the average molar mass values and of molar mass distributions determined by MS. ESI-MS analysis gives complementary information to other methods of analysis, such as SEC and NMR spectroscopy. SEC is the most widely used method to determine molar mass [31]. It separates polymers according to their hydrodynamic volume, V_h [32, 33], which depends on both molar mass and branching [34]. This may lead to incomplete SEC separation in terms of molar mass due to branching [35-37]. Multiple-detection SEC can be used to detect LCBs [20]. This method allows determination of the local number- and weight-average molar

mass as well as the local dispersity of molar mass at each elution volume $Đ(V_h)$ [34]. The local dispersity assesses the accuracy of the determined molar mass [11] but it provides only an indirect assessment of the heterogeneity of the macromolecular structure due to branching. In the case of PAA, aqueous and organic SEC provide different molar mass values [12] due to the presence of branches.

In further work, poly(sodium acrylate)s (PNaAs) were separated by free-solution capillary electrophoresis (CE) according to their branching topology with limited influence of the molar mass [7]. Indeed, for homopolyelectrolytes, such as poly(sodium acrylate) [29, 38] above around 10 monomer units, the analysis is undertaken in the critical conditions. This does not refer to a separation mode but to the conditions sought in liquid chromatography in which polymers are not separated according to their molar mass [39, 40]. The electrophoretic mobility increases as *DB* decreases [7, 41]. Capillary electrophoresis in the critical conditions (CE-CC) can thus separate polyelectrolytes according to their microstructure and allow characterization of the heterogeneity of branching. By heterogeneity, we mean that different macromolecules within the same samples can differ by their branching, namely number of branches per macromolecule, but also position of the respective branching points along the polymer chain, distribution of molar masses of the branches etc. CE-CC was used in this work to determine the dispersity of the electrophoretic mobility distributions. As different branching topologies lead to different electrophoretic mobilities in the case of poly(sodium acrylate), the obtained values of dispersity are representative of the heterogeneity of branching [41].

The aim of this study was to characterize the structure of PAA (synthesized by conventional radical polymerization) by ESI-MS, solution-state NMR spectroscopy and CE-CC. From these three methods, the influence of different parameters – temperature, initial monomer concentration and presence of CTA – on the chemical structure of PAA was determined in order to better understand the mechanism and kinetics of polymerization.

2. Experimental section

2.1. Materials

Acrylic acid (AA, 99%), 4,4’-azobis(4-cyanovaleric acid) (75%+) and thioglycolic acid (98%) were supplied by Sigma-Aldrich. Deuterium oxide (99.9% D), NaOD (40% in D_2O) and DCl (35% in D_2O) were supplied by Cambridge Isotope Laboratory Inc. Traces of PAA were found in the deuterium oxide at the last stage of the experimental work. The effect of the contamination on this study was tested and results are available in the supplementary data (Figures S15 and S16). Methanol (analytical grade) was supplied by Merck. Tetrahydrofuran (THF, HPLC grade) was passed through a solvent purification system [42].

Acetonitrile and methanoic acid (analytical grade) were provided by Fluka. Water was of Milli-Q quality. Boric acid (≥ 98%) was purchased from BDH AnalaR, Merck Pty Ltd. Sodium hydroxide pellets and dimethyl sulfoxide, DMSO, were supplied by Sigma Chemical Company. One PAA sample was received from Sigma-Aldrich (catalog number: 026C; lot number: 100416003). The linear PNaA was obtained from PSS (Mainz, Germany), as described in [7].

4,4'-azobis(4-cyanovaleric acid) was used as received. Thioglycolic acid and acrylic acid were distilled under reduced pressure.

2.2. Synthesis

Into a 50 mL Schlenk round-bottom flask were added 12.4 mg of 4,4'-azobis(4-cyanovaleric acid) (to give a concentration of 2.00×10^{-3} mol L^{-1} for polymerization), 3.00 mL of acrylic acid (1.99 mol L^{-1} for polymerization), 0.0 or 0.3 mL of thioglycolic acid (0.0 or 0.2 mol L^{-1} for polymerization) and 22 mL of solvent (H_2O/THF 8/2 v/v). This solvent mixture was chosen because it has been found to be efficient for chain transfer to thioglycolic acid [43]. The amount of CTA was chosen in order to obtain a DP_n close to 10, and thus facilitate analysis of these (short) polymers by ESI-MS. The Schlenk round bottom flask was degassed by bubbling nitrogen through the solution for 30 min. The mixture was left under stirring at 50, 70 or 90 °C for 24 h, 6 h or 1 h, respectively. After these reactions times, the samples were quenched in ice water. THF was evaporated using a rotary evaporator and the remaining aqueous solution was freeze-dried for 48 h. Then, a white powder was collected. Polymerization at 90 °C without CTA was repeated with different amounts of solvent (14.6 mL and 44 mL, corresponding to 3.00 mol L^{-1} and 0.99 mol L^{-1}, respectively, of acrylic acid) in order to study the influence of the initial monomer concentration on the structure of the polymer. Reaction times were chosen to give high conversion (see Table S1). The monomer conversions were shown to be higher than 88 % by both ^{1}H NMR spectroscopy and CE (see Figure S2 and Table S2).

2.3. Mass spectrometry

2 different operators performed the ESI MS analyses: one run the PAA samples synthesized at 70 and 90 °C (operator a) and the second one the PAA sample synthesized at 50 °C (operator b).

The samples for ESI-MS analysis were prepared as follows: 1 mg of PAA was dissolved in 1 mL of

water/methanol (1/1 v/v). The samples were injected into a Thermo Fisher Scientific Dionex UltiMate 3000 liquid chromatography (LC) system (without a column) comprised of an Ultimate 3000 RS Pump, 3000 RS Autosampler, 3000 RS Column Compartment, 3000 Diode Array Detector. The LC system was attached to a Bruker maXis 3G Ultra High Resolution Time of Flight tandem mass spectrometer (Bruker Daltonics). The isocratic mobile phase comprised 0.1% (v/v) formic acid and 50% (v/v) acetonitrile in water at a flow rate of 300 µL min^{-1} (operator a) and 200 µL min^{-1} (operator b). Ions were generated by electrospray ionization (ESI) and cleaned of solvent by a nitrogen flow of 8.0 L min^{-1}, temperature of 200 °C, nebulizer at 1 bar, end plate offset at 500 V, capillary voltage at 4000 V, and analysis in positive-ion mode. The intensity of positive ions was recorded in the range of 30–2414 m/z (operator a) and 100-3000 m/z (operator b), at a rate of 2 s^{-1} and analysed using Bruker Compass HyStar 3.2 – SR 2 (Build 44). The voltage peak to peak was 3000 Vpp (operator a) and 1200 Vpp (operator b).

2.4. NMR spectroscopy

Spectra of PAAs synthesized by conventional radical polymerization with and without CTA were acquired in D_2O at 26 °C (^1H NMR spectra) or 49 °C (^{13}C NMR spectra) on an Agilent 400 MR with Varian 7600-AS auto-sampler, equipped with a OneNMR probe and variable temperature capabilities, operating at Larmor frequencies of 399.84 MHz for ^1H and 100.55 MHz for ^{13}C. The presence of thioglycolic acid during the synthesis is expected to influence the chain length and *DB*. The solubility of the PAAs in D_2O and the signal to noise ratios (*SNRs)* of the peak of the quaternary carbon thus vary, and so some conditions of analysis (number of scans, concentration of PAA in D_2O) were adjusted for each sample. The polymer concentrations for ^{13}C NMR analyses are given in Table S5. For the ^1H NMR analyses, a few mg of PAA were dissolved in a few tenths of mL of D_2O. The volume of D_2O was measured with a plastic syringe. One-dimensional ^1H NMR spectra were acquired with 16,384 data points, 128 scans, 16 ppm spectral width (6,410.3 Hz), 40 s relaxation delay, 2.556 s acquisition time and a 90° flip angle. One-dimensional ^{13}C NMR spectra were recorded with 32,768 data points, 16,500 to 19,000 scans, 246.8 ppm spectral width (25,000 Hz), 10.0 s relaxation delay and a 90° flip angle with inverse-gated decoupling. The chemical shift scales were calibrated for ^1H and ^{13}C NMR spectra by measuring spectra of acrylic acid with methanol in D_2O. The ^1H and ^{13}C NMR signal assignments are provided in Tables S7 and S8, and examples of the NMR spectra are shown in Figures S3 to S6. In order to assign each peak, 2D COSY and HSQC NMR experiments were carried out (see Figure S7).

One-dimensional T_1-relaxation time experiments have determined that a relaxation delay of 10.0 s with an acquisition time of 1.311 s is sufficient to ensure quantitative results (acquisition time + relaxation

delay > 5 × T_1) (see Figure S8). The inversion recovery experiment was carried out with one value of τ between the two pulses. Another inversion recovery experiment established that a 6.5 s relaxation delay with a 1.311 s acquisition time is insufficient for a full recovery of these signals (see Figure S9). The inversion recovery experiments are described in detail in the supplementary data. Estimations of the T_1 of the C_q signal are given in table S9.

DB was quantified in percentage of monomer units by comparing the integrals, *I*, of C_q at 48 ppm and of the main chain CH at 39-42 ppm as follows:

$$DB(\%) = \frac{100 \cdot I(\mathrm{C_q})}{I(\mathrm{C_q}) + I(\mathrm{CH})} \quad (1)$$

For thiol-containing PAA, the carbon called C_{thiol}, meaning the carbon of the CH adjacent to the thioglycolic acid end group-residue (i.e. adjacent to the sulfur atom), exhibited a signal at 44 ppm. This is overlapping with the main-chain CH signal (see Figure S6). An over- and underestimation of *DB* were calculated as follows for thiol-containing PAA. For the overestimation, the integral of the CH signal excluded the contribution of the overlapping C_{thiol} signal by setting the left integration limit to the valley between the C_{thiol} and CH signals (Eq. (2)). For the underestimation, the integral of the CH signal included the contribution of the overlapping C_{thiol} signal by setting the left integration limit to the left of the C_{thiol} signal (Eq. (3)).

$$DB_{overestimate}(\%) = \frac{100 \cdot I(\mathrm{C_q})}{I(\mathrm{C_q}) + I(\mathrm{CH})_{\text{excluding overlapping } \mathrm{C_{thiol}}}} \quad (2)$$

$$DB_{underestimate}(\%) = \frac{100 \cdot I(\mathrm{C_q})}{I(\mathrm{C_q}) + I(\mathrm{CH})_{\text{including overlapping } \mathrm{C_{thiol}}}} \quad (3)$$

The signal of C_q of in the ^{13}C NMR spectrum of PAA synthesized at 50 °C without CTA was observed with a *SNR* < 3, which is the limit of detection (LOD). To have an estimate of a "potential" maximum degree of branching, the *SNR* of the main chain CH signal and the one of the C_q signal were compared (see Eq. (S2) and (S3)).

The PAA from Sigma Aldrich was analyzed at room temperature on a Bruker DRX300 spectrometer (Bruker, Biospin Ltd, Sydney) equipped with a 5 mm dual $^1H/^{13}C$ probe at Larmor frequencies of 300.13 MHz for ^1H and 75 MHz for ^{13}C NMR. The PAA provided by Sigma-Aldrich was dissolved at 27 g L^{-1} in D_2O (with 1 mol equivalent of NaOD to the carboxylic acid unit and 0.5 mol equivalent of DCl to the

carboxylic acid unit). A one-dimensional ^{1}H NMR spectrum was acquired with 8 scans, 5.0 s acquisition time + relaxation delay, and 30° flip angle. A one-dimensional ^{13}C NMR spectrum was recorded with 27,411 scans, 5.8 s relaxation delay, 0.2 s acquisition time and a 90° flip angle, with inverse-gated decoupling. One-dimensional T_1-relaxation time experiments have determined that a relaxation delay of 5.8 s with an acquisition time of 0.2 s would be sufficient to ensure quantitative results (acquisition time + relaxation delay > 5 T_1). As the signal of the main-chain CH was overlapping with the signal of the main-chain CH_2, *DB* was calculated by comparing the integral of the signal of quaternary carbon to that of the carboxylic acid group, as follows:

$$DB(\%) = \frac{100 \cdot I(C_q)}{I(COOH)} \qquad (4)$$

This equation was also used to obtain another estimate of *DB* for all samples of this work (Table S9).

The relative standard deviation (*RSD*) of *DB* (in percent of *DB* values) was calculated from the signal-to-noise ratio (*SNR*) of the quaternary carbon C_q using Eq. (5), which was established for branching measurements in polyethylene by combination of both derivation from calculation error and empirical results [44] and assessed to be accurate also for branching measurements in hydrophobic polyacrylates [20].

$$RSD = \frac{238}{SNR^{1.28}} \qquad (5)$$

2.5. Capillary electrophoresis

The instrument and conditions were as in [7]. The preparation of a 110 mM sodium borate buffer at pH 9.2 was as in [7]. For each sample, 10 mg of PAA were dissolved in 1.5 mL of Milli-Q water with a small volume of sodium hydroxide solution (15 µL, 1 mol L^{-1} in Milli-Q water). 500 µL of dissolved PNaA were mixed with 10 µL of 10 wt. % aqueous DMSO (added as an electroosmotic flow marker). Each sample was diluted several times with Milli-Q water until repeatable normalized electrophoretic mobility distributions at two successive concentrations were obtained (see Table S11 as well as Figures S18 and S19). The separations were performed with a high sensitivity, 50 µm internal diameter fused-silica capillary (Agilent, Australia) with a total length of 62.2 cm and an effective length of 53.7 cm at 30 kV and 25 °C. The electrophoretic mobility distributions and their dispersities were calculated from the raw electropherograms, as in [41] (see also Eq. (S10) to (S13)). Electrophoretic mobility is preferred to

migration time because it is more repeatable and it characterizes the topology of polymers [39]. The pH of each PNaA sample before injection was measured to be between 4 and 5 (using a pH meter). In order to check if incomplete dissolution due to low pH influences the electropherograms, the samples were titrated until pH > 8 and CE experiments were repeated in similar conditions. Electrophoretic mobility distributions of PNaA dissolved at acidic and basic pH are reproducible in terms of shape and electrophoretic mobility (Figure S20). However, an effect on the peak area of the electropherogram exists. This issue will not be discussed at this stage. Data was treated with the Origin 9.0 software. The pH meter was a SevenCompact™ pH/Ion meter S220 (Mettler Toledo), calibrated with internal standards with pH values of 4, 7 and 9.2 or 4, 7 and 10.

3. Results and discussion

The PAAs synthesized in the presence and in the absence of thiol were characterized in terms of end groups, chain length and branching. They were compared to other PAAs (or PNaAs). Table 1 summarizes all polymers used to carry out this study and how they were synthesized.

Table 1: Summary of all polymerizations used to carry out this study

Polymer	Synthesis method	Reactants (Initiator/CTA/monomer/solvent)	Conversion	M_n
PAAs specifically synthesized for this study (without CTA)	Conventional radical polymerization	ACVA/No CTA/Acrylic acid/water THF (v/v 8/2)	> 94 %*	unknown
PAAs specifically synthesized for this study (with CTA)	Conventional radical polymerization	ACVA/thioglycolic acid/Acrylic acid/water THF (v/v 8/2)	> 88 %*	Unknown (but the DP_ns are expected to be close to 10 at 65 °C)
PAA provided by sigma Aldrich	unknown	unknown	unknown	240,000 $g.mol^{-1}$ #
Linear PNaA[7]	Anionic polymerization	*t*-butyl acrylate	unknown	39,300 $g.mol^{-1}$
Hyperbranched PAA[7]	Nitroxide mediated	Alkoxyamine/SG1/acrylic acid/1,4-dioxane	50 %	12,300 $g.mol^{-1}$

	polymerization			

*: the monomer conversion of AA was estimated using ^{1}H NMR spectroscopy and CE (See Table S2 and Figure S1.

#: from the supplier, determination method not given.

3.1. End groups by ESI-MS

Figure 1 shows the mass spectra of PAAs synthesized with thiol at 50, 70 and 90 °C. When synthesized without CTA, no peaks were observed, as high molar mass components tend to ionize poorly [45]. When the PAA is synthesized at 70 °C with CTA, the number-average degree of polymerization, DP_n, is expected to be about 10 [43] (i.e. number-average molar mass, M_n, of about 813 g.mol^{-1}, this being the molar mass of 10 acrylic acid units inserted into a thioglycolic acid molecule).

According to the ESI-MS spectra, the majority of the species have the same end groups (HOOC-CH_2-S of CTA at one end and H at the other). The different families of peaks observed for the PAA obtained at 50, 70 and 90 °C correspond to different adducts. The main observed adducts are HOOC-CH_2-S-$(AA)_n$-H H^+, HOOC-CH_2-S-$(AA)_n$-H NH_4^+, and HOOC-CH_2-S-$(AA)_n$-H Na^+. Doubly charged adducts were observed in the spectrum of thiol-containing PAA synthesized at 70 °C and 90 °C. Tables S2, S3 and S4 detail the different adducts and compare their observed *m*/*z* with the theoretical value calculated with the mMass software (version 3.1.0). [46] The average size of the polymer is, of course, reduced by transfer from propagating radicals to a CTA. No terminal double bond was detected in the polymers obtained at any of the three polymerization temperatures, which is a similar trend to the the results of Junkers *et al.*, who found that the presence of a CTA reduces the amount of β-scission in poly(alkyl acrylates) [27]. This should also apply to PAA.

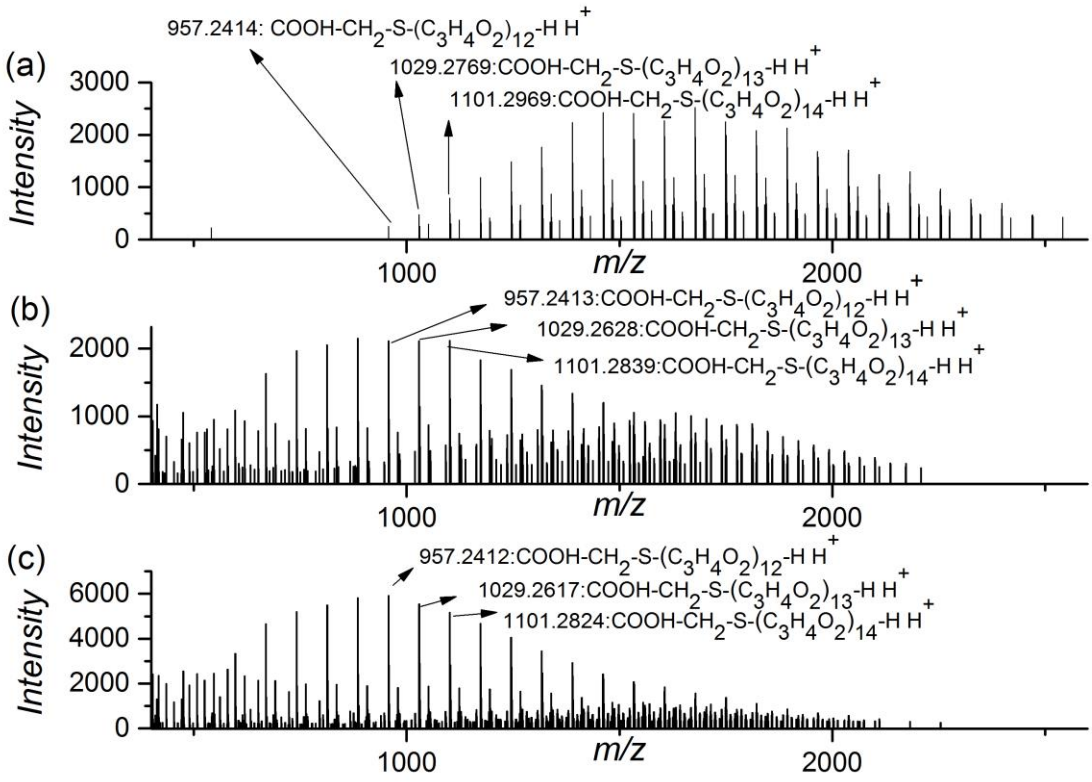

Figure 1: ESI mass spectra of thiol-containing PAAs synthesized at (a) 50 °C, (b) 70 °C, and (c) 90 °C.

3.2. Determination of the average degree of branching

As the PAAs synthesized by conventional radical polymerization and the PAA provided by Sigma were analyzed in different conditions (temperature and pH), the influence of these physical parameters on the required time for precise, quantitative measurement of *DB* by ^{13}C NMR spectroscopy was studied.

The temperature and magnetic field of the NMR spectroscopy analysis, as well as the electronic configuration of the analyzed molecule – the PAA provided by Sigma was analyzed as PNaA – influence the relaxation delay, T_1, of its nuclei. When the molecule is charged and the temperature is lower, T_1 decreases. A repetition delay of 6 s was sufficient to have quantitative results when PAA was analyzed at room temperature and with NaOD, whilst a repetition delay of 7.811 s was insufficient to obtain a quantitative ^{13}C NMR spectrum of PAA when analyzed at 49 °C in D_2O without NaOD. At room temperature and with 27,411 scans, a higher *SNR* is observed than at 49 °C with 17,500 scans, but the resolution is lower (see Figures S11 and S12). Table S6 sums up all the conditions for analyses of

branching in PAA or PNaA by ^{13}C NMR spectroscopy that have been reported in the literature. The *SNR* of the C_q peak is never given in the literature and the time of analysis is not always mentioned. Moreover, even when it is claimed that the analyses are quantitative, the T_1 measurement experiment is not always mentioned, while it is the only way to know whether or not the conditions for quantitative analysis are met. Consequently, it was not possible to determine the optimal conditions of analyses based on literature. Figure 2 shows the partial ^{13}C NMR spectra of PAAs synthesized at 90 °C with and without CTA.

The different values obtained for *DB* (with Eq. (1), (2), (3) and (4)) are similar (and in the same range if the *RSD* is taken into account). The dissolution of polymers is a process whose complexity is regularly underestimated.[47, 48] For example in the case of starch, transparent liquids resisting to centrifugation were shown by NMR spectroscopy to still be incompletely dissolved.[49] Some inaccuracies of *DB* measurement could be due to incomplete dissolution of PAA in D_2O (especially for the CTA-containing PAAs). The solubility of PAA in D_2O was tested by comparing the ^{13}C NMR spectra of different PAAs using the normalized peak area to noise ratio, defined as follows.

The "peak area to noise ratio" (*PNR*) of a NMR signal is defined as the absolute peak area divided by the noise. It is relevant to study the dissolution of a sample in the deuterated solvent as the peak area is used as the quantity proportional to the amount of sample and the noise as the scaling factor to put all spectra on the same scale. The normalized *PNR* corresponds to the *PNR* of a signal divided by the PAA label concentration used for the NMR measurement and by the square root of the number of scans (Eq. (S4) was used). Both main chain CH and COOH signals were used in this instance. The normalized *PNR* of COOH and CH signals in all PAAs synthesized by conventional radical polymerization were compared to the normalized *PNR* of the same signals in the linear PNaA (which is assumed to be fully soluble in D_2O). Results are presented in Figure S13. Similar calculations were carried out using the *SNR* instead of the *PNR*. Results are presented in Figure S14. However, *PNR* is preferred to *SNR* as it is not demonstrated that the height of the signal is proportional to the amount of sample.

In the case of PAAs synthesized with CTA, a significantly lower normalized *PNR* than in the case of the linear PNaA is observed for both COOH and CH backbone signals, which suggests that they are less dissolved in D_2O. This could be due to the presence of sulfur in the end group. Consequently, *DB* values obtained for these two samples may be less accurate than the ones measured in the other PAAs.

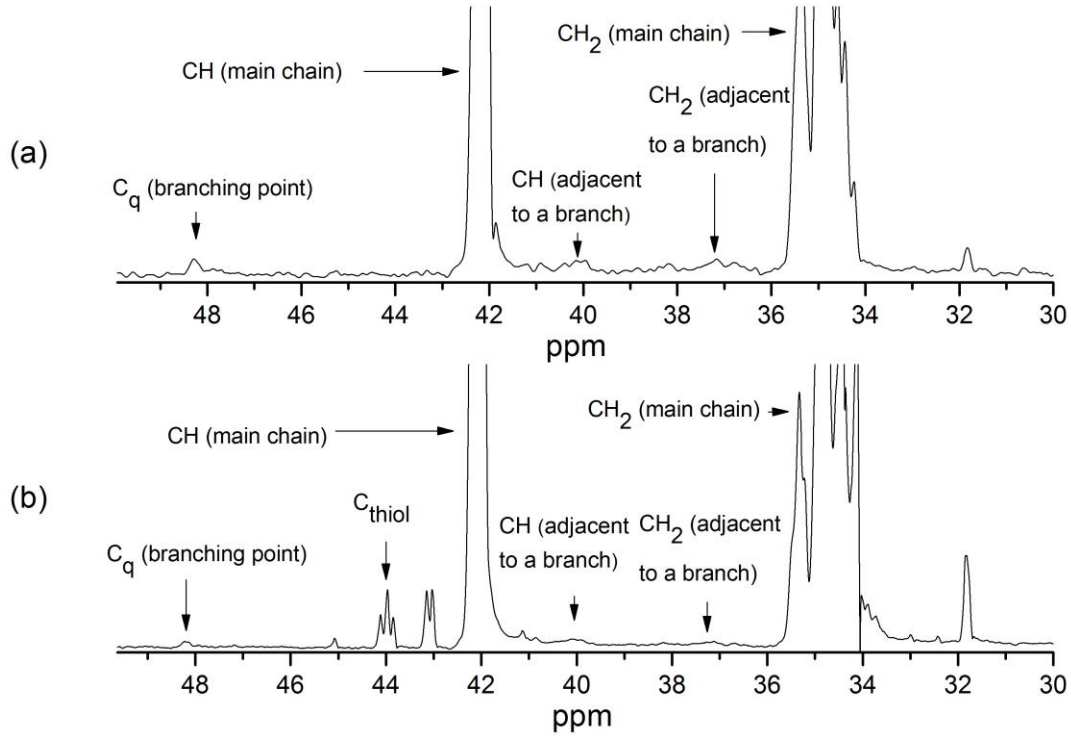

Figure 2: Partial ^{13}C solution-state NMR spectra in D_2O at 49 °C of PAA synthesized at 90 °C (a) without CTA and (b) with CTA.

3.3. Values of the average *DB*

*DB*s obtained for CTA-containing polymers are significantly lower than the ones obtained in conventional systems at 70 °C and 90 °C (Figure 3b). Thus the CTA reduces not only the average chain length of the polymer but also *DB*. Of course reduction of average chain length also reduces the number of branches per chain, as observed in PLP [27]. However, *DB* is expressed per monomer unit and not per chain, and so the reduction of *DB* is a different phenomenon, as conventional transfer to CTA does not change the macroradical concentration and consequently should not change the frequency of transfer to polymer reactions. One likely explanation is the patching effect of tertiary MCRs by CTA, as postulated for poly(*n*-butyl acrylates) [17]. Another possible explanation for the reduction of *DB* due to the presence of a CTA is the lowering of the number of backbiting events in comparison to propagation of SPRs [21, 50], since the time of polymerization is shorter for the PAA synthesized in the presence of the CTA. This difference might also be exacerbated by unintended temperature increase. Although in laboratory experiments like these one strives to maintain constant temperature, the polymerizations

were performed in round-bottom flasks with magnetic stirring and the fast rates of acrylate polymerizations sometimes give rise to an exotherm, even in relatively dilute solution. In the absence of CTA, chains will be longer, and hence solutions more viscous. This makes heat transfer more difficult, and hence exotherm effects more likely. Such would give an enhancement of *DB*, as observed.

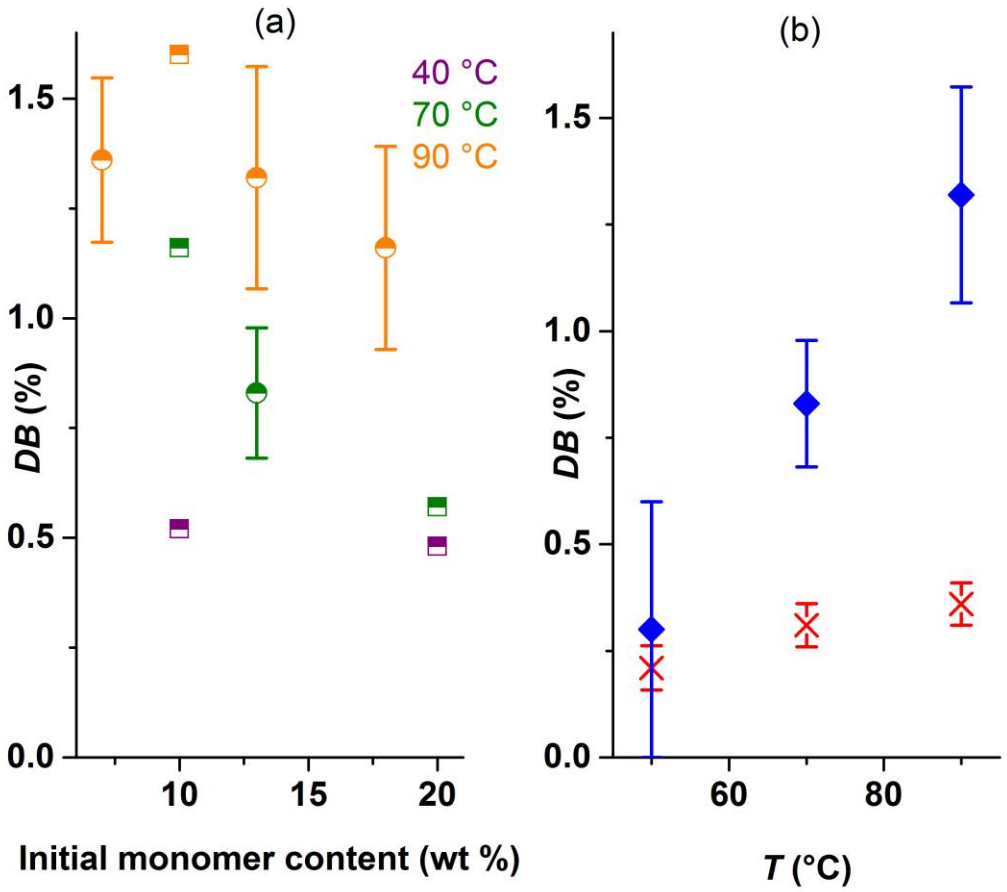

Figure 3: Average degree of branching, *DB*, in percent of monomer units, as a function of: (a) initial monomer concentration: results from Wittenberg are represented by semi-filled squares and results from this study by semi-filled circles; and (b) synthesis temperature for PAA synthesized in solution without (blue diamonds) or with (red crosses) 0.2 mol L^{-1} CTA. *DB*s of CTA-containing polymers presented in this graph were calculated with Eq. (2). *DB*s of non-CTA containing PAAs were calculated with Eq. (1) (except for the PAA synthesized at 50 °C without CTA, where Eq. (S2) was used).

DB increases with the temperature. This can be explained by the increase of frequencies of the reactions that lead to MCRs, viz. inter- and intramolecular (chain) transfer. Typical activation energies of these transfer reactions are between 20 and 25 kJ mol^{-1} higher than that of chain-end (as opposed to mid-chain) propagation in the case of alkyl acrylates [13]. Wittenberg *et al.* tabulated the activation energy of backbiting and chain-end propagation steps for polymerization of non-ionized acrylic acid as being 38

and 13 kJ mol^{-1} respectively [18]. These values were calculated for batch radical polymerization of 5 to 40% non-ionized acrylic acid in aqueous solution between 40 °C and 90 °C. In this study, the temperatures and monomer concentration are within the same range but acrylic acid was polymerized in water/THF (8/2 v/v)), also in batch. Thus conditions were essentially the same, apart from having 20% THF as solvent rather than 100% water.

Figure 3b shows that as temperature is increased, the effect of CTA on *DB* becomes stronger, i.e. there is a bigger gap between *DB* with and without CTA: at 50 °C there is no difference within the limit of detection, but at 90 °C the value with 0.2 mol L^{-1} CTA is about one third of what it is without. An obvious explanation for this is that the patching reaction becomes more prominent as the temperature increases.

Wittenberg *et al.* [18] also quantified *DB* of PAA produced by radical polymerization in water without CTA at high conversion (> 95 %) in a similar range of temperatures (40 °C to 90 °C). Their results (*DB* from 0.48 % to 1.60 %) are close to the ones in this study (and are in the same range taking the error bars into account). Figure 4 provides a comparison between *DB* obtained for PAA synthesized without CTA in this study and in the study by Wittenberg *et al*. The *DB*s are of the same magnitude between both sets of work, for polymer obtained under similar conditions and analysed with the same solvent, D_2O, in ^{13}C NMR. It is important to note that, although Wittenberg *et al.* carried out AA polymerizations in the presence of 2-mercaptoethanol, they do not appear to have measured *DB* in such experiments, rather just the molar mass distributions (by size exclusion chromatography) and conversion as a function of time (by infrared spectroscopy). Nevertheless, the fact that our *DB*s from PAAs synthesized without CTA are in such good agreement gives confidence that *DBs* given by Wittenberg *et al*. are obtained without CTA.

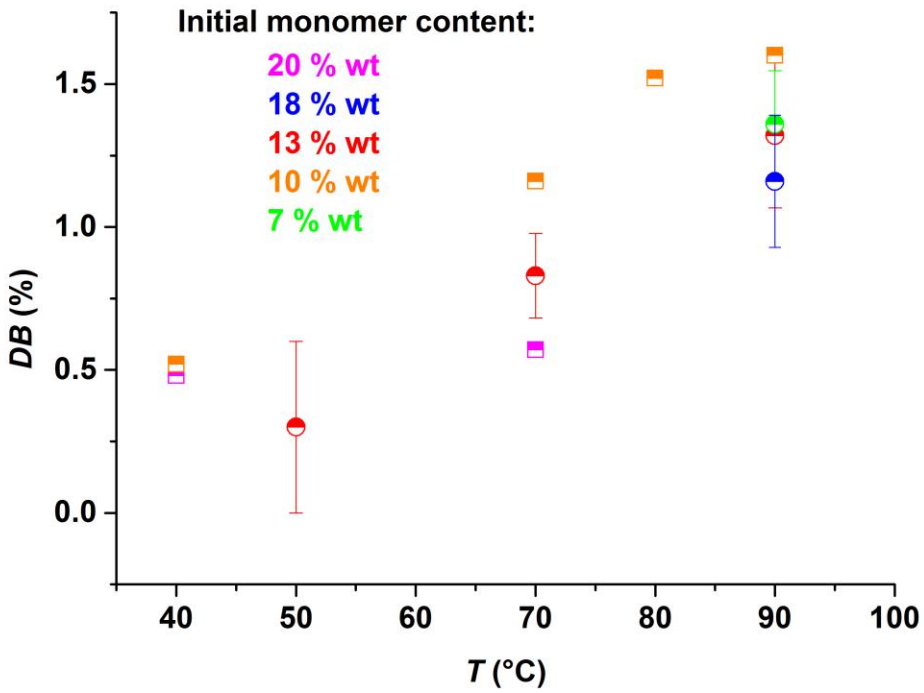

Figure 4: *DB* of PAAs synthesized by conventional radical polymerization in aqueous solution without CTA: comparison between the results obtained in this study (semi-filled circles) and results obtained by Wittenberg *et al.* (semi-filled squares) [18]. In both studies *DB* is from the whole polymer present near the end of a batch polymerization.

Turning again to Figure 3b, at 50 °C the results are different to 70 °C and 90 °C: the presence of the CTA does not reduce *DB* as at the other temperatures (within experimental error). At 50 °C, poly(acrylic acid) radicals might not transfer as efficiently to thioglycolic acid. The lower likelihood of exotherm effects at 50 °C, where the polymerization is slower than at 70 and 90 °C, could also be playing a role (see earlier discussion).

The present *DB*s – for PAA synthesized in water/THF (8/2 v/v) – are lower than for poly(*n*-butyl acrylate) (PnBA) synthesized in bulk by Gaborieau *et al.* between 60 and 140 °C. To be precise, these PnBAs have *DB*s of 2 to 5 % when synthesized without CTA and 0.7 to 2 % when synthesized with CTA.[17] Both these minimum values are lower than those obtained at 90 °C in this work (see Figure 3b). This could possibly be explained by a lower rate of intermolecular chain transfer when polymers are in dilute solution: polymers do not overlap and consequently *DB* is reduced. Dilution by water also favors the propagation through an entropic effect: the strong hydrogen bonding between the water and the propagating radicals creates disorder (thus lowering the pre-exponential factor of the propagation rate

coefficient) [51]. The propagation rate coefficient of AA was observed both experimentally and theoretically to strongly increase with dilution by water. Dilution and H-bonding may also reduce the formation of branching points (by intramolecular transfer to polymer). As water forms H-bonding with the carboxylic group of the acrylic acid unit, the dilution by water could explain the discrepancy between this work and results from Gaborieau et *al*.. However, the most likely explanation for the lower *DB* is simply that backbiting relative to propagation is slower in AA than in *n*-butyl acrylate.

The initial monomer concentration does not seem to have any influence on *DB* (Figure 3a). Indeed, *DB*s at initial [AA] = 1 mol L^{-1}, 2 mol L^{-1} and 3 mol L^{-1} (which correspond to 7.3 to 18.1 wt.%) are comparable. As explained previously, the chain length, which depends on the monomer concentration, does not directly influence *DB*. Rather, it confirms the assumption that *DB* does not decrease with the chain length. The initial monomer concentration may influence the number of branches per chain but not the number of branches per monomer unit. The monomer conversion could also play a role here, as the rates of polymerization and of branch formation depend on the monomer conversion: the cumulative *DB* is expected to increase significantly when above 90 % monomer conversion[18, 52]. The syntheses at initial monomer concentrations of 1, 2 and 3 mol L^{-1} may not have led to exactly the same monomer conversion. According to Wittenberg et al.'s simulations, even a small difference of conversion above 90 °C would lead to different *DB*s. As the syntheses of PAAs at 3 different monomer concentrations were carried out using the same reaction time, this is quite possible. Another issue that could lead to these results is an exotherm. As explained previously, this issue becomes more important in viscous solutions, and could explain the results observed at different monomer concentrations (the increase in monomer content leads to more viscous solutions). Another explanation can be based on observations by Lovell *et al.* at high conversion (on *n*-butyl acrylate) [19] and Loiseau *et al.* for the RAFT polymerization of acrylic acid [6]: branches can result from intermolecular chain transfer to polymer reactions, whose rate does not depend on the initial monomer concentration as soon as the polymer concentration is above the critical overlapping concentration, *c**. Since all the syntheses of PAA without CTA have been done mostly above *c**, there is thus the possibility of intermolecular chain transfer, leading to *DB* roughly independent of initial monomer concentration. Of course backbiting is assumed to dominate in most cases, especially in PLP (even if LCB was detected for poly(alkyl acrylates) obtained by PLP [11]). It cannot be affirmed that the branching is mostly due to intermolecular transfer to polymer. Finally, as the relative standard deviation of *DB* of PAAs synthesized at 90 °C without CTA is quite large (up to 20 %), the precision of these results is relatively limited. Some variations of *DB*, lower than 20%, may exist.

Wittenberg *et al.* observed potentially different results. When the polymerization occurs at 40 °C and 70 °C, a potential decrease in *DB* is observed when the initial monomer concentration is increased from 10 to 20 wt.% [18]. This is in line with expectation: as monomer concentration is increased, the frequency of propagation (a bimolecular process) is increased whereas the frequency of backbiting (a unimolecular process) remains unchanged, and thus the fraction of branches decreases. This has been observed in most other works, and thus doubt is cast on the present results for *DB* as a function of initial [AA]. However, as the standard deviation is not given by Wittenberg *at al.*, it is impossible to know whether or not their observed differences are significant. Moreover, it is not proven that their ^{13}C NMR analyses are quantitative (it was not shown that the repetition delay was greater than $5T_1$).. The presence of a non-soluble fraction, whose branching would not be detected and quantified by solution-state NMR, could also play a role.

The present results were compared with *DB* of a PAA provided by Sigma Aldrich. This PAA has an expected number average molar mass M_n = 240 000 g mol^{-1} (it is however to be noted that determination of PAA molar mass suffers from a poor accuracy [12, 31]). A *DB* was measured in this work as 1.13 ± 0.07 %. This value is in the same range as *DB*s of PAAs synthesized by conventional radical polymerization without CTA, which suggests that it may have been synthesized using similar experimental conditions.

3.4. Backbiting rates coefficients

Assuming, reasonably, that the loss of MCRs by transfer (in the absence of transfer agent), β-scission and termination by disproportionation is negligible, then every backbiting event leads to a branching point, and thus the fraction of branching points is given by the ratio of the rate of backbiting to the rate of propagation. The rate of propagation is not constant during a polymerization but Nikitin et al. were able to link the DB to the ratio of the backbiting to the propagation rate coefficients as in Eq. (6):

$$DB\ (\%) = \frac{k_{\mathrm{bb}}\ 100\ (\ln([\mathrm{M}]_0/([\mathrm{M}]_{\mathrm{e}})}{k_{\mathrm{p}}\ ([\mathrm{M}]_0 - ([\mathrm{M}]_{\mathrm{e}})} \qquad (6)$$

Where $[\mathrm{M}]_0$ is the initial monomer concentration and $[\mathrm{M}]_{\mathrm{e}}$ is the final monomer concentration. Thus from a measurement of *DB* one can very easily obtain $k_{\mathrm{bb}}/k_{\mathrm{p}}$, where this k_{p} refers to chain-end (secondary-radical) propagation. Wittenberg *et al.* [18] were able to use an even simpler expression since they used low-conversion conditions in their particular experiments to determine $k_{\mathrm{bb}}/k_{\mathrm{p}}$ from *DB*. In the present case our results are from batch polymerization in which conversion traversed from 0 % to

nearly 100 % and equation (6) is thus used instead. If one uses *DB* values of similar precision and accuracy, then Wittenberg et al.'s expression should lead to more accurate values since it is not impacted by the uncertainty on the determination of the conversion.

To obtain individual values of k_{bb}, the value of k_p was needed. This was calculated using Eq. (S6) given in [18], which is re-estimated from an earlier PLP-SEC study on non-ionized AA [53]

Figure 5 is an Arrhenius plot for k_{bb} obtained in both the presence and absence of CTA in water/THF (8/2 v/v) compared with the Arrhenius equation tabulated by Wittenberg *et al.* [18] and Barth *et al.*[54]. Wittenberg *et al*.'s equation was obtained by combining their k_{bb} from a handful of low-conversion *DB* (from polymerization in pure water) with a larger data set from Barth *et al.* [54], who used single pulse - pulsed laser polymerization - electron paramagnetic resonance (SP-PLP-EPR) spectroscopy experiments to determine k_{bb}, also at low-conversion conditions. These experiments involve monitoring of EPR signals on a microsecond timescale over which the conversion of chain-end radicals into MCRs can be observed. Eqs. (8), (9) and (S8) represent, respectively, the Arrhenius fits for k_{bb} calculated from *DB*s of this study in both the absence and presence of CTA; and from Wittenberg *et al.* at low conversion [54]. The linear fits parameters are presented in table S11. The linear fit for the PAA obtained in this work in the absence of CTA gave a Pearson's R^2 coefficient of 0.56 only with the point for the polymerization at 90 °C and 1 M monomer concentration looking like an outlier. This point was removed and the Pearson's R^2 coefficient increased to 0.996. The parameters for both fits are given in Table S11, but only the fit excluding 1 M monomer concentration is given on figure 5. The *RSD* of ln k_{bb} was calculated based on the *RSD* of *DB*, according to Eq. (S9), which assumes that the error on k_{bb} only depends on the error on *DB*. The error is not visible on the graph as it is negligible (between 4×10^{-7} and 4×10^{-4}). This high precision is distinct from the accuracy of these measurements, which is likely lower than in previous works due to the high monomer conversion.

.

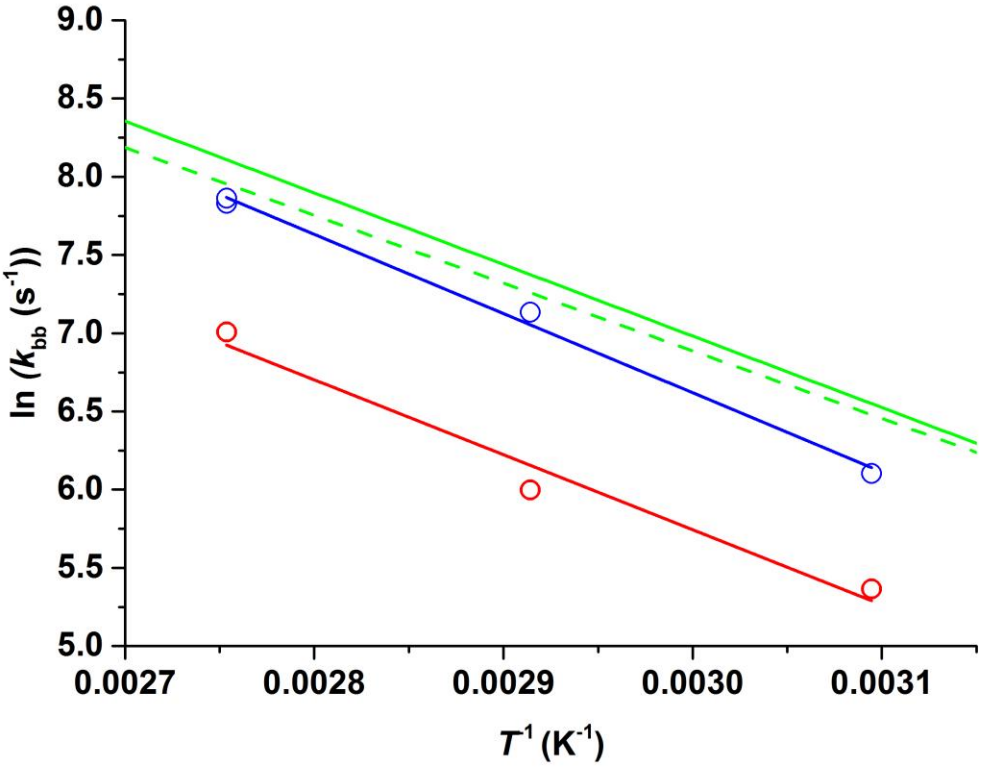

Figure 5: Arrhenius plot of k_{bb} in absence of CTA (blue line and points), presence of CTA (red line and points) and from Wittenberg *et al.*[18] (full green line) and Barth et al [54](dashed green line).

$$k_{bb}\ (s^{-1}) = 2.99\ \times\ 10^{9}\ (s^{-1})\ e^{-\frac{5066}{T/K}} \tag{8}$$

$$k_{bb}\ (s^{-1}) = 5.20\ \times\ 10^{8} (s^{-1})\ e^{-\frac{4777}{T/K}} \tag{9}$$

In Figure 5 the (apparent) activation energy of k_{bb} is similar in the presence of CTA. The pre-exponential factor is, however, lower in the presence of CTA. As previously explained, the presence of CTA might reduce the number of backbiting steps as the macroradical polymerizes for a shorter time [21]. Another hypothesis is the invalidity of Eq. (6) in the presence of CTA. Given that a patching effect is possible some MCRs could not lead to a branched chain, thus *DB* would not be directly related to k_{bb}. In effect this is a breakdown of the assumption that all MCRs undergo propagation rather than any other reaction (see above).

The k_{bb} values observed in this study in the absence of CTA are a bit more than 170 % lower than the ones determined by Wittenberg *et al.* Several explanations are possible. First, the observed differences

could just be due to different systematic error (for example due to incomplete dissolution in some cases). Second, the high conversion in this work leads to a lower accuracy of the determined k_{bb} values for at least three potential reasons: (i) the uncertainty on the value of the monomer conversion, (ii) the non-validity of the assumption that k_p is constant, (iii) intermolecular chain transfer to polymer may not be negligible. . In the case of Wittenberg *et al.*, the conditions to obtain quantitative *DB* values were not checked and the *RSD* of *DB* was not provided at all.

On Figure S17 no proportionality between *DB* and $1/[M]_0$ is observed.

3.5. Heterogeneity of branching

While the average *DB* has been determined for PAAs obtained in a number of different polymerization conditions in this work and in the literature, the variation of *DB* from macromolecule to macromolecule within a given sample has not been examined. CE-CC provides important information related to the heterogeneity of branching. This heterogeneity is not just due to different *DB*s within a sample but also different positions of the branching points or a distribution of molar masses of the branches. As polymers are separated according to their topology and not according to their size in CE-CC, the dispersity of the distribution of electrophoretic mobilities is related to the heterogeneity of branching [41]. It is in contrast with SEC with which polymers are separated according to their hydrodynamic volume [32] (which depends on both the molar mass and the branching). Multiple-detection SEC allows measurement of local weight- and local number-average molar mass as well as their ratio $Đ(V_h)$. Values of the local dispersity $Đ(V_h)$ (of the local molar mass distribution) primarily inform the accuracy of the determined molar mass but also provide indirect information on the heterogeneity of branching. In the case of poly(alkyl acrylates), the most heterogeneous samples (in terms of branching) were shown to be obtained for low *DB*s [11, 20]. Multiple-detection SEC is however not only an indirect characterization method for the branching, but also a tedious method. Free-solution CE allows much higher throughput and simple characterization of the branching [7, 39]. The dispersity of the electrophoretic mobility distributions was calculated in this work as a standard deviation [56], and as a ratio of four moments of the mobility distribution [41]. The dispersities of the distributions of electrophoretic mobilities $D(W(\mu),1,0)$, $D(W(\mu),2,0)$, $D(W(\mu),3,0)$ and D_σ were calculated according to Eq. (S10) to (S13) [41]. $D(W(\mu),1,0)$ is calculated as the ratio of the first and zeroth order moments divided by the ratio of the zeroth and -1st order moments. It is in analogy with M_w/M_n where M_w is the weight-average molar mass. $D(W(\mu),2,0)$ is calculated as the ratio of the second and first order moments divided by the ratio of the first and zeroth order moments. It is in analogy with M_z/M_w where M_z is the z-average molar mass.

$D(W(\mu),3,0)$ is calculated as the ratio of the third and second order moments divided by the ratio of the second and first order moments. The last dispersity D_σ is calculated as a standard deviation of the weight distribution of electrophoretic mobilities. The weight-average electrophoretic mobility μ_W is the equivalent of the weight-average molar mass in term of electrophoretic mobility. μ_W is determined as the ratio of the first and zeroth order moments of the mobility distributions and is given by Eq. (S14) [41]. The values of the different dispersities and of the μ_W of the different PNaAs are given in Table S13.

The electrophoretic mobility distributions of branched PNaA exhibit two peaks (see Figure 6) that are not resolved. This is not the case for the linear PNaA, whose electropherogram exhibits only one peak. The bimodal shape of branched PNaA was already observed in previous work [7, 41]. The relation between the polymer structure and it electrophoretic mobility can be undertaken using a "slope plot"[57] but this beyond the scope of this work. The dispersities of electrophoretic mobility distributions were calculated on the whole distributions of electrophoretic mobilities in order to assess the heterogeneity due to branching in each individual PNaA sample. As a DP_n around 10 is expected for the PAAs synthesized at 50 °C, 70 °C and 90 °C with CTA [43], their separation and analysis by capillary electrophoresis are not expected to be in the critical conditions and are thus not considered in this study of the heterogeneity of branching (the distributions are broader in the case of CTA-containing polymers than non-CTA containing polymer, as observed in figures S18 and S19 due to the combined influences of molar mass and branching).

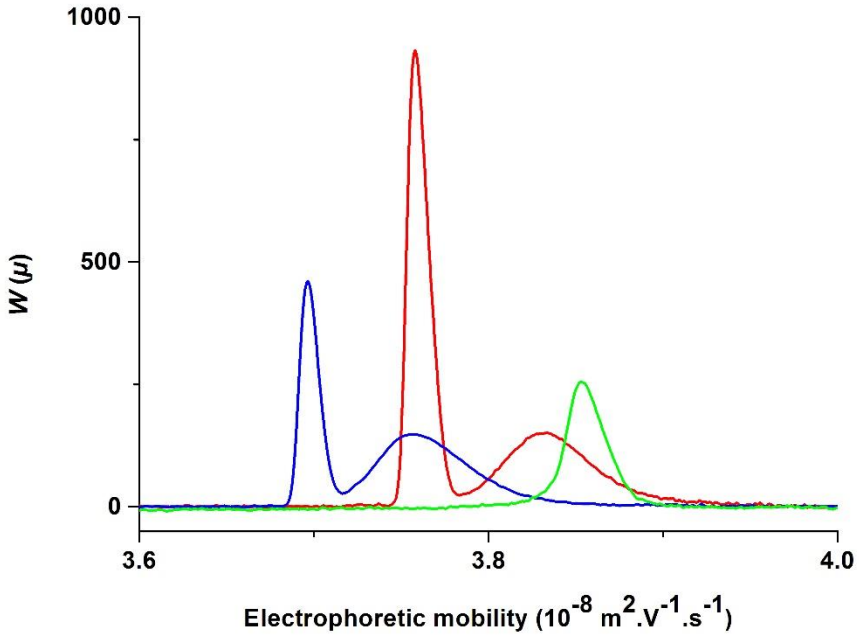

Figure 6: Electropherograms of PAAs synthesized without CTA at 70 °C (red line,) 90 °C (blue line) and a linear PNaA (green line). All samples are analyzed as PNaAs at high pH.

Figure 7 shows that neither the temperature nor the initial monomer concentration influences significantly the heterogeneity of branching of the 3 PNaAs obtained by conventional radical polymerization at different temperatures and monomer concentrations. When the PNaA is synthesized without CTA, high enough *DB*s may be obtained for the branching to be relatively homogeneous which would explain the similar heterogeneity of branching with the temperature and the initial monomer concentration.

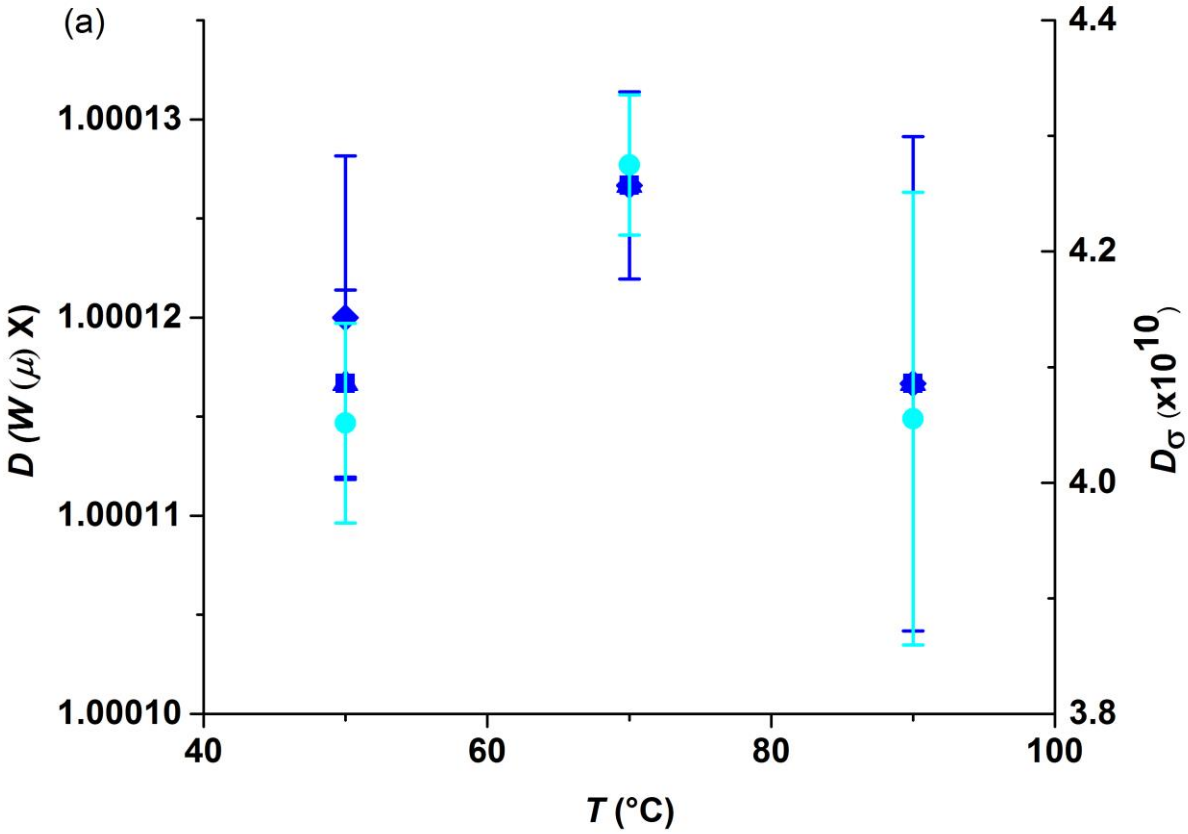
(a)
1.00013
1.00012
1.00011
1.00010
D (W (μ) X)
40
60
80
100
T (°C)
4.4
4.2
4.0
3.8
Dσ (x10^10)

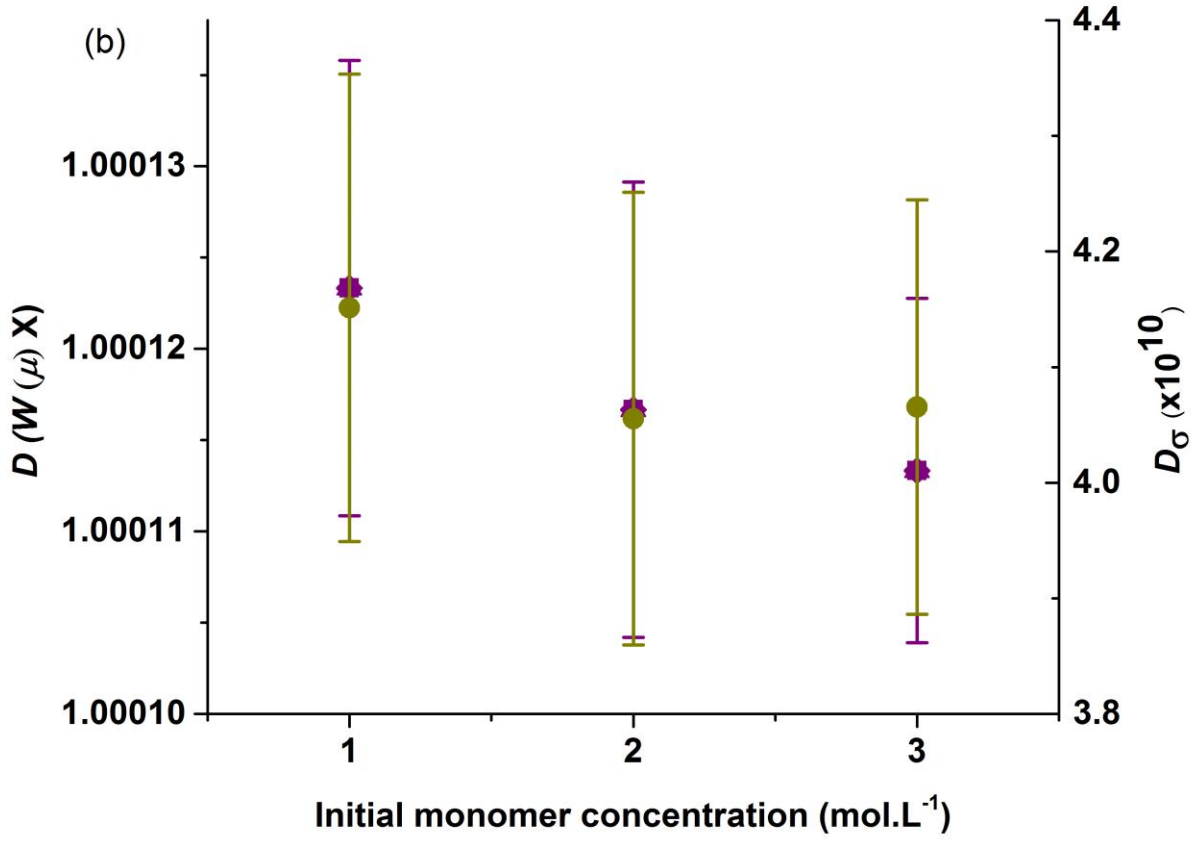

Figure 7: Dispersities $D(W(\mu), x, 0)$ of electrophoretic mobility distributions of PNaAs as a function of (a) synthesis temperature (all PAAs synthesized without CTA at $[M]_0$ = 2 mol L^{-1}), (b) initial monomer concentration (all PAAs synthesized at 90 °C). x = 1:■; x = 2:▲; x = 3:◆; D_σ:●.

The evolution of the dispersity of electrophoretic mobility distributions with *DB* is shown on Figure 8. The dispersity of electrophoretic mobility distributions of the PNaAs produced by conventional radical polymerization is compared with those of the linear PNaA and of a hyperbranched PNaA [41] produced by nitroxide-mediated polymerization in the presence of an alkoxyamine inimer, leading to a *DB* estimated at 3.9 ± 0.1 %. The synthesis of the hyperbranched PNaA is described elsewhere in detail [7]. The linear PNaA has the lowest heterogeneity of branching as all chains are unbranched (the dispersity should be equal to unity, the lowest value possible, as no heterogeneity from branching is expected). The heterogeneity of branching of the hyperbranched PNaA (produced by controlled polymerization and with a *DB* of 3.9 ± 0.1 %) is higher than the ones observed for the PNaAs produced by conventional radical polymerization. When PNaAs are produced by conventional radical polymerization, branching

results only from inter and intramolecular (chain) transfer to polymer. Only LCB and SCB are expected. Branching initiated by the inimer is also expected in the case of the hyperbranched PNaA, which may explain the higher heterogeneity. A higher $Đ(V_h)$ was also observed for poly(alkyl acrylates) produced by controlled radical polymerization than by conventional radical polymerization [37]. The dispersities determined in this work should relate to the local dispersities $Đ(V_h)$ which could also be determined by multiple-detection SEC but have not been reported in the literature for PAA or PNaA. The lowest dispersity of the electrophoretic mobility distribution should correspond to the lowest $Đ(V_h)$ and thus the most accurate determined molar mass. The higher dispersities observed for PNaAs produced by radical polymerization can be explained by branching and is one likely cause of the low accuracy of the molar mass of PNaA (or PAA, or equivalent) determined by SEC [12]. Figure 9 shows the evolution of the dispersity with μ_w, and confirms that the more a polyelectrolyte is branched, the lower the mobility is. The same phenomenon as in Figure 7 is observed. The hyperbranched PNaA produced by controlled radical polymerization has the highest dispersity of the electrophoretic mobility distributions and, as the highest *DB*, the lowest mobility and the linear PNaA which has no branches has the highest mobility (as expected).

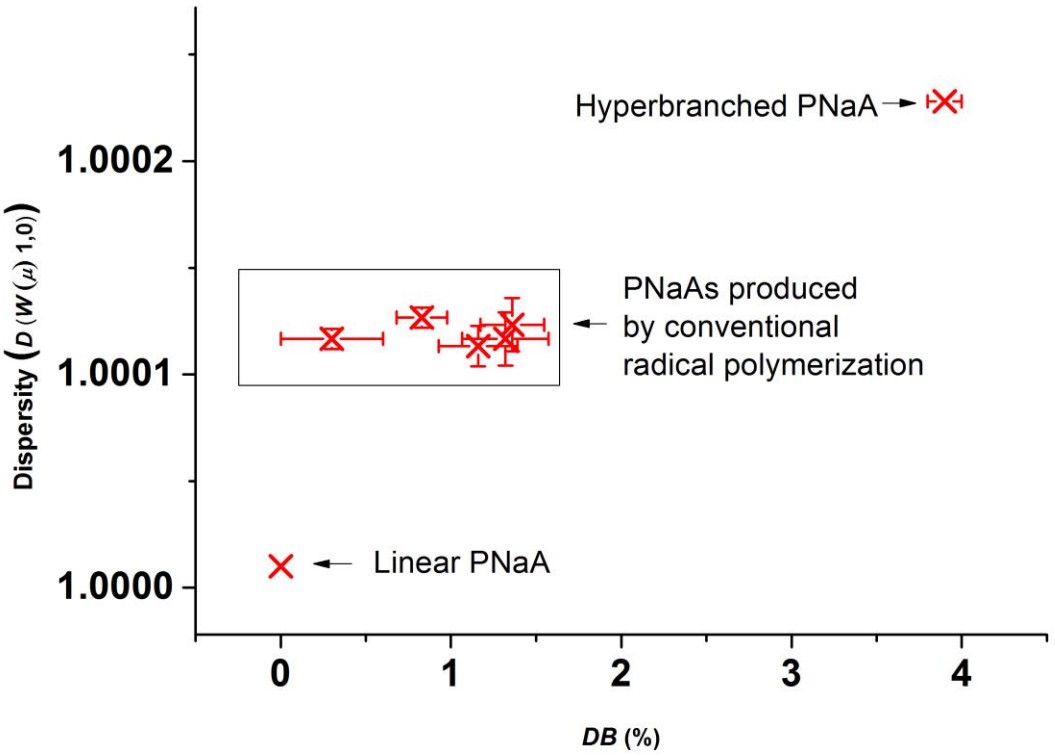

Figure 8: Dispersity $D(W(\mu),1,0)$ of the electrophoretic mobility distributions of PNaAs as a function of their average *DB*.

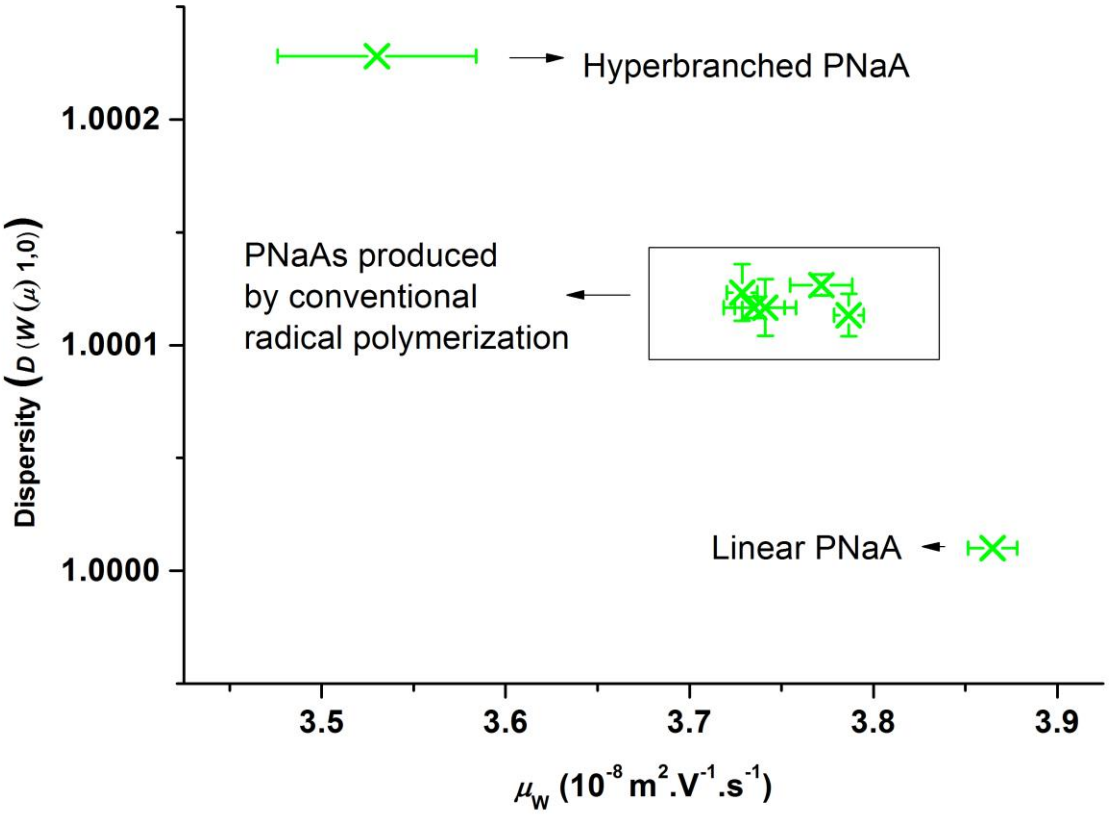

Figure 9: Dispersity $D(W(\mu),1,0)$ of the electrophoretic mobility distributions of PNaAs as a function of the weight-average electrophoretic mobility μ_W.

4. Conclusion

In this paper, *DB* was measured with quantitative ^{13}C solution-state NMR spectroscopy and the heterogeneity of branching was measured by CE-CC. These were both done for PAA synthesized in both the presence and absence of thioglycolic acid at various temperatures and initial monomer concentrations. The presence of thiol decreases *DB,* the so-called "patching effect" is observed for PAA, exactly as it has been for other acrylic monomers. However, the reduction in *DB* may also be due to a decrease of the number of backbiting steps in comparison to propagation steps. *DB* was observed to increase with the temperature. This is due to an acceleration of the reactions which lead to the formation of branching points (transfer to polymer). When PAA is synthesized at 90 °C without a CTA, the initial monomer concentration (1, 2 and 3 mol L^{-1}) does not appear to influence the degree or the heterogeneity of branching, although this observation for *DB* is not commensurate with other

observations, both in this work and in the literature. This might be due to unintended temperature increase over the polymerization process, slight differences in monomer conversion, or the limited precision of the analyses. PAA produced by conventional radical polymerization is not only branched, but different macromolecules within a sample are branched differently. The heterogeneity of branching observed for a linear PNaA is negligible, as it should, and lower than the one of the PNaAs synthesized by conventional radical polymerization, which is in turn lower than the one of the hyperbranched PNaA (synthesized by nitroxide-mediated polymerization). The heterogeneity increases with the diversity of branching structures. Moreover, it is confirmed that the electrophoretic mobility decreases with the increase of branching. This work provides relevant information for a systematic variation of reaction conditions that can be used for future kinetic and mechanistic studies, which will help to optimize conditions for poly(acrylic acid) synthesis in numerous applications.

5. Acknowledgements

We thank Dr Chris Fellows (University of New England), Adam Sutton (University of South Australia) and Cedric Loubat (Specific Polymer Ltd) for their feedback related to this research. We thank the Macromolecular Characterization Team (WSU) for their help in the lab with CE, Dr Ghislain David (Ecole Nationale Superieure de Chimie de Montpellier) for providing very useful information related to the synthesis of PAA, Dr Matthew Polson (UC) for assistance in the laboratory, Dr Marie Squire (UC) for help with NMR spectroscopy and ESI-MS and Dr Sarah Masters (UC) for help with proof-reading. JBL thanks the University of Canterbury for a UC Doctoral Scholarship and general research support from the Evans Fund.

References

[1] X.H. Xu, B. Bai, C.X. Ding, H.L. Wang, Y.R. Suo, Synthesis and properties of an ecofriendly superabsorbent composite by grafting the poly(acrylic acid) onto the surface of dopamine-coated sea buckthorn branches, Ind. Eng. Chem. Res. 54 (2015) 3268-3278, 10.1021/acs.iecr.5b00092.

[2] B. Bolto, J. Gregory, Organic polyelectrolytes in water treatment, Water Res. 41 (2007) 2301-2324, 10.1016/j.watres.2007.03.012.

[3] S.F. Duan, S. Cai, Y.M. Xie, T. Bagby, S.Q. Ren, M.L. Forrest, Synthesis and characterization of a multiarm poly(acrylic acid) star polymer for application in sustained delivery of cisplatin and a nitric oxide prodrug, J. Polym. Sci. A Polym. Chem. 50 (2012) 2715-2724, 10.1002/pola.26059.

[4] L.A. Connal, Q. Li, J.F. Quinn, E. Tjipto, F. Caruso, G.G. Qiao, PH-responsive poly(acrylic acid) core cross-linked star polymers: Morphology transitions in solution and multilayer thin films, Macromolecules 41 (2008) 2620-2626, 10.1021/ma7019557.

[5] A.D. Wallace, A. Al-Hamzah, C.P. East, W.O.S. Doherty, C.M. Fellows, Effect of poly(acrylic acid) end-group functionality on inhibition of calcium oxalate crystal growth, J. Appl. Polym. Sci. 116 (2010) 1165-1171, 10.1002/app.31657.

[6] J. Loiseau, N. Doerr, J.M. Suau, J.B. Egraz, M.F. Llauro, C. Ladaviere, Synthesis and characterization of poly(acrylic acid) produced by RAFT polymerization. Application as a very efficient dispersant of CaCO3, kaolin, and TiO2, Macromolecules 36 (2003) 3066-3077, 10.1021/ma0256744.

[7] A.R. Maniego, D. Ang, Y. Guillaneuf, C. Lefay, D. Gigmes, J.R. Aldrich-Wright, M. Gaborieau, P. Castignolles, Separation of poly(acrylic acid) salts according to topology using capillary electrophoresis in the critical conditions, Anal. Bioanal. Chem. 405 (2013) 9009-9020, 10.1007/s00216-013-7059-y.

[8] L. Couvreur, C. Lefay, J. Belleney, B. Charleux, O. Guerret, S. Magnet, First nitroxide-mediated controlled free-radical polymerization of acrylic acid, Macromolecules 36 (2003) 8260-8267, 10.1021/ma035043p.

[9] P.M. Wood-Adams, J.M. Dealy, A.W. deGroot, O.D. Redwine, Effect of molecular structure on the linear viscoelastic behavior of polyethylene, Macromolecules 33 (2000) 7489-7499, 10.1021/ma991533z.

[10] C. Barner-Kowollik, S. Beuermann, M. Buback, P. Castignolles, B. Charleux, M.L. Coote, R.A. Hutchinson, T. Junkers, I. Lacik, G.T. Russell, M. Stach, A.M. van Herk, Critically evaluated rate coefficients in radical polymerization - 7. Secondary-radical propagation rate coefficients for methyl acrylate in the bulk, Polym. Chem. 5 (2013) 204-212, 10.1039/C3PY00774J.

[11] P. Castignolles, Transfer to polymer and long-chain branching in PLP-SEC of acrylates, Macromol. Rapid Commun. 30 (2009) 1995-2001, 10.1002/marc.200900530.

[12] I. Lacík, M. Stach, P. Kasák, V. Semak, L. Uhelská, A. Chovancová, G. Reinhold, P. Kilz, G. Delaittre, B. Charleux, I. Chaduc, F. D'Agosto, M. Lansalot, M. Gaborieau, P. Castignolles, R.G. Gilbert, Z. Szablan, C. Barner-Kowollik, P. Hesse, M. Buback, SEC analysis of poly(acrylic acid) and poly(methacrylic acid), Macromol. Chem. Phys. 216 (2015) 23-37, 10.1002/macp.201400339.

[13] T. Junkers, C. Barner-Kowollik, The role of mid-chain radicals in acrylate free radical polymerization: Branching and scission, J. Polym. Sci. A Polym. Chem. 46 (2008) 7585-7605, 10.1002/pola.23071.

[14] A.N. Nikitin, P. Castignolles, B. Charleux, J.P. Vairon, Determination of propagation rate coefficient of acrylates by pulsed-laser polymerization in the presence of intramolecular chain transfer to polymer, Macromol. Rapid Commun. 24 (2003) 778-782, 10.1002/marc.200350025.

[15] M. Buback, P. Hesse, I. Lacik, Propagation rate coefficient and fraction of mid-chain radicals for acrylic acid polymerization in aqueous solution, Macromol. Rapid Commun. 28 (2007) 2049-2054, 10.1002/marc.200700396.

[16] K.B. Kockler, A.P. Haehnel, T. Junkers, C. Barner-Kowollik, Determining Free-Radical Propagation Rate Coefficients with High-Frequency Lasers: Current Status and Future Perspectives, Macromol. Rapid Commun. 37 (2016) 123-134, 10.1002/marc.201500503.

[17] M. Gaborieau, S.P.S. Koo, P. Castignolles, T. Junkers, C. Barner-Kowollik, Reducing the degree of branching in polyacrylates via midchain radical patching: A quantitative melt-state NMR study, Macromolecules 43 (2010) 5492-5495, 10.1021/ma100991c.

[18] N.F.G. Wittenberg, C. Preusser, H. Kattner, M. Stach, I. Lacík, R.A. Hutchinson, M. Buback, Modeling acrylic acid radical polymerization in aqueous solution, Macromol. React. Eng. 10 (2016) 95-107, 10.1002/mren.201500017.

[19] N.M. Ahmad, F. Heatley, P.A. Lovell, Chain transfer to polymer in free-radical solution polymerization of n-butyl acrylate studied by NMR spectroscopy, Macromolecules 31 (1998) 2822-2827, 10.1021/ma0101299.

[20] P. Castignolles, R. Graf, M. Parkinson, M. Wilhelm, M. Gaborieau, Detection and quantification of branching in polyacrylates by size-exclusion chromatography (SEC) and melt-state 13C NMR spectroscopy, Polymer 50 (2009) 2373-2383, 10.1016/j.polymer.2009.03.021.
[21] N. Ballard, J.C. de la Cal, J.M. Asua, The role of chain transfer agent in reducing branching content in radical polymerization of acrylates, Macromolecules 48 (2015) 987-993, 10.1021/ma502575j.
[22] B. Wenn, G. Reekmans, P. Adriaensens, T. Junkers, Photoinduced acrylate polymerization: Unexpected reduction in chain branching, Macromol. Rapid Commun. 36 (2015) 1479-1485, 10.1002/marc.201500198.
[23] N.M. Ahmad, B. Charleux, C. Farcet, C.J. Ferguson, S.G. Gaynor, B.S. Hawkett, F. Heatley, B. Klumperman, D. Konkolewicz, P.A. Lovell, K. Matyjaszewski, R. Venkatesh, Chain transfer to polymer and branching in controlled radical polymerizations of n-butyl acrylate, Macromol. Rapid Commun. 30 (2009) 2002-2021, 10.1002/marc.200900450.
[24] S. Hamzehlou, N. Ballard, Y. Reyes, A. Aguirre, J.M. Asua, J.R. Leiza, Analyzing the discrepancies in the activation energies of the backbiting and beta-scission reactions in the radical polymerization of n-butyl acrylate, Polym. Chem. 7 (2016) 2069-2077, 10.1039/c5py01990g.
[25] T. Caykara, O. Guven, Effect of preparation methods on thermal properties of poly(acrylic acid) silica composites, J. Appl. Polym. Sci. 70 (1998) 891-895, 10.1002/(sici)1097-4628(19981031)70:5<891::aid-app8>3.0.co;2-o.
[26] C. Barner-Kowollik, T.P. Davis, M.H. Stenzel, Probing mechanistic features of conventional, catalytic and living free radical polymerizations using soft ionization mass spectrometric techniques, Polymer 45 (2004) 7791-7805, 10.1016/j.polymer.2004.09.017.
[27] T. Junkers, S.P.S. Koo, T.P. Davis, M.H. Stenzel, C. Barner-Kowollik, Mapping poly(butyl acrylate) product distributions by mass spectrometry in a wide temperature range: Suppression of midchain radical side reactions, Macromolecules 40 (2007) 8906-8912, 10.1021/ma071471+.
[28] S.P.S. Koo, T. Junkers, C. Barner-Kowollik, Quantitative product spectrum analysis of poly(butyl acrylate) via electrospray ionization mass spectrometry, Macromolecules 42 (2009) 62-69, 10.1021/ma801196w.
[29] M. Gaborieau, T.J. Causon, Y. Guillaneuf, E.F. Hilder, P. Castignolles, Molecular weight and tacticty of oligoacrylates by capillary electrophoresis - mass spectrometry, Aus. J. Chem. 63 (2010) 1219-1226, 10.1071/CH10088.
[30] C.M. Guttman, K.M. Flynn, W.E. Wallace, A.J. Kearsley, Quantitative mass spectrometry and polydisperse materials: Creation of an absolute molecular mass distribution polymer standard, Macromolecules 42 (2009) 1695-1702, 10.1021/ma802199r.
[31] D. Berek, Size exclusion chromatography - A blessing and a curse of science and technology of synthetic polymers, J. Sep. Sci. 33 (2010) 315-335, 10.1002/jssc.200900709.
[32] Z. Grubisic, P. Rempp, H. Benoit, A universal calibration for gel permeation chromatography, J. Polym. Sci. B Polym. Lett. 5 (1967) 753-759, 10.1002/pol.1967.110050903.
[33] Z. Grubisic, P. Rempp, H. Benoit, A universal calibration for gel permeation chromatography (Reprinted from Polymer Letters, vol 5, pg 753-759, 1967), J. Polym. Sci. B Polym. Phys. 34 (1996) 1707-1713, 10.1002/polb.1996.922.
[34] M. Gaborieau, P. Castignolles, Size-exclusion chromatography (SEC) of branched polymers and polysaccharides, Anal. Bioanal. Chem. 399 (2011) 1413-1423, 10.1007/s00216-010-4221-7.
[35] L.K. Kostanski, D.M. Keller, A.E. Hamielec, Size-exclusion chromatography - a review of calibration methodologies, J. Biochem. Biophys. Methods 58 (2004) 159-186, 10.1016/j.jbbm.2003.10.001.

[36] M. Gaborieau, R.G. Gilbert, A. Gray-Weale, J.M. Hernandez, P. Castignolles, Theory of multiple detection size exclusion chromatography of complex branched polymers, Macromol. Theory Simul. 16 (2007) 13-28, 10.1002/mats.200600046.
[37] M. Gaborieau, J. Nicolas, M. Save, B. Charleux, J.P. Vairon, R.G. Gilbert, P. Castignolles, Separation of complex branched polymers by size-exclusion chromatography probed with multiple detection, J. Chromatogr. A 1190 (2008) 215-223, 10.1016/j.chroma.2008.03.031.
[38] P. Castignolles, M. Gaborieau, E.F. Hilder, E. Sprong, C.J. Ferguson, R.G. Gilbert, High-resolution separation of oligo(acrylic acid) by capillary zone electrophoresis, Macromol. Rapid Commun. 27 (2006) 42-46, 10.1002/marc.200500641.
[39] J.J. Thevarajah, M. Gaborieau, P. Castignolles, Separation and characterization of synthetic polyelectrolytes and polysaccharides with capillary electrophoresis, Adv. Chem. 2014 (2014) Article ID 798503, 10.1155/2014/798503.
[40] M. Rollet, B. Pelletier, A. Altounian, D. Berek, S. Maria, E. Beaudoin, D. Gigmes, 86 (2014) 2694,
[41] J.J. Thevarajah, A.T. Sutton, A.R. Maniego, E.G. Whitty, S. Harrisson, H. Cottet, P. Castignolles, M. Gaborieau, Quantifying the heterogeneity of chemical structures in complex charged polymers through the dispersity of their distributions of electrophoretic mobilities or of compositions, Anal. Chem. 88 (2016) 1674-1681, 10.1021/acs.analchem.5b03672.
[42] A.B. Pangborn, M.A. Giardello, R.H. Grubbs, R.K. Rosen, F.J. Timmers, Safe and convenient procedure for solvent purification, Organometallics 15 (1996) 1518-1520, 10.1021/om9503712.
[43] C. Loubat, B. Boutevin, Telomerization of acrylic acid with thioglycolic acid - Effect of the solvent on the C-T value, Polym. Bull. 44 (2000) 569-576, 10.1007/s002890070080.
[44] K. Klimke, M. Parkinson, C. Piel, W. Kaminsky, H.W. Spiess, M. Wilhelm, Optimisation and application of polyolefin branch quantification by melt-state 13C NMR spectroscopy, Macromol. Chem. Phys. 207 (2006) 382-395, 10.1002/macp.200500422.
[45] J.A. Leenheer, C.E. Rostad, P.M. Gates, E.T. Furlong, I. Ferrer, Molecular resolution and fragmentation of fulvic acid by electrospray ionization/multistage tandem mass spectrometry, Anal. Chem. 73 (2001) 1461-1471, 10.1021/ac0012593.
[46] M. Strohalm, “mMass - Open Source Mass Spectrometry Tool”, http://www.mmass.org/, accessed: February 2013.
[47] B.A. Miller-Chou, J.L. Koenig, A review of polymer dissolution, Prog. Polym. Sci. 28 (2003) 1223-1270, 10.1016/s0079-6700(03)00045-5.
[48] J.J. Thevarajah, J.C. Bulanadi, M. Wagner, M. Gaborieau, P. Castignolles, Towards a less biased dissolution of chitosan, Anal. Chim. Acta 935 (2016) 258-268, 10.1016/j.aca.2016.06.021.
[49] S. Schmitz, A.C. Dona, P. Castignolles, R.G. Gilbert, M. Gaborieau, Assessment of the extent of starch dissolution in dimethyl sulfoxide by 1H NMR spectroscopy, Macromol. Biosci. 9 (2009) 506-514, 10.1002/mabi.200800244.
[50] N. Ballard, J. Ignacio Santos, J.M. Asua, Reevaluation of the formation and reactivity of midchain radicals in nitroxide-mediated polymerization of acrylic monomers, Macromolecules 48 (2015) 2909-2915, 10.1021/acs.macromol.5b00347.
[51] I. Degirmenci, T.F. Ozaltin, O. Karahan, V. Van Speybroeck, M. Waroquier, V. Aviyente, Origins of the solvent effect on the propagation kinetics of acrylic acid and methacrylic acid, J. Polym. Sci. A Polym. Chem. 51 (2013) 2024-2034, 10.1002/pola.26589.
[52] A.N. Nikitin, R.A. Hutchinson, G.A. Kalfas, J.R. Richards, C. Bruni, The Effect of Intramolecular Transfer to Polymer on Stationary Free-Radical Polymerization of Alkyl Acrylates, 3-Consideration of Solution Polymerization up to High Conversions, 18 (2009) 247-258, 10.1002/mats.200900009.

[53] I. Lacik, S. Beuermann, M. Buback, Aqueous phase size-exclusion-chromatography used for PLP-SEC studies into free-radical propagation rate of acrylic acid in aqueous solution, Macromolecules 34 (2001) 6224-6228, 10.1021/ma002222n.

[54] J. Barth, W. Meiser, M. Buback, SP-PLP-EPR study into termination and transfer kinetics of non-ionized acrylic acid polymerized in aqueous solution, Macromolecules 45 (2012) 1339-1345, 10.1021/ma202322a.

[55] D. Cuccato, E. Mavroudakis, M. Dossi, D. Moscatelli, A density functional theory study of secondary reactions in n-butyl acrylate free radical polymerization, Macromol. Theory Simul. 22 (2013) 127-135, 10.1002/mats.201200079.

[56] J. Chamieh, M. Martin, H. Cottet, Quantitative analysis in capillary electrophoresis: Transformation of raw electropherograms into continuous distributions, Anal. Chem. 87 (2015) 1050-1057, 10.1021/ac503789s.

[57] A. Ibrahim, S.A. Allison, H. Cottet, Extracting Information from the Ionic Strength Dependence of Electrophoretic Mobility by Use of the Slope Plot, 84 (2012) 9422-9430, 10.1021/ac302033z.

[58] A.R. Maniego, A.T. Sutton, Y. Guillaneuf, C. Lefay, M. Destarac, C.M. Fellows, P. Castignolles, M. Gaborieau, Characterization of branching in poly(acrylic acid) prepared by controlled and conventional radical polymerization, Manuscript in preparation.

Graphical abstract

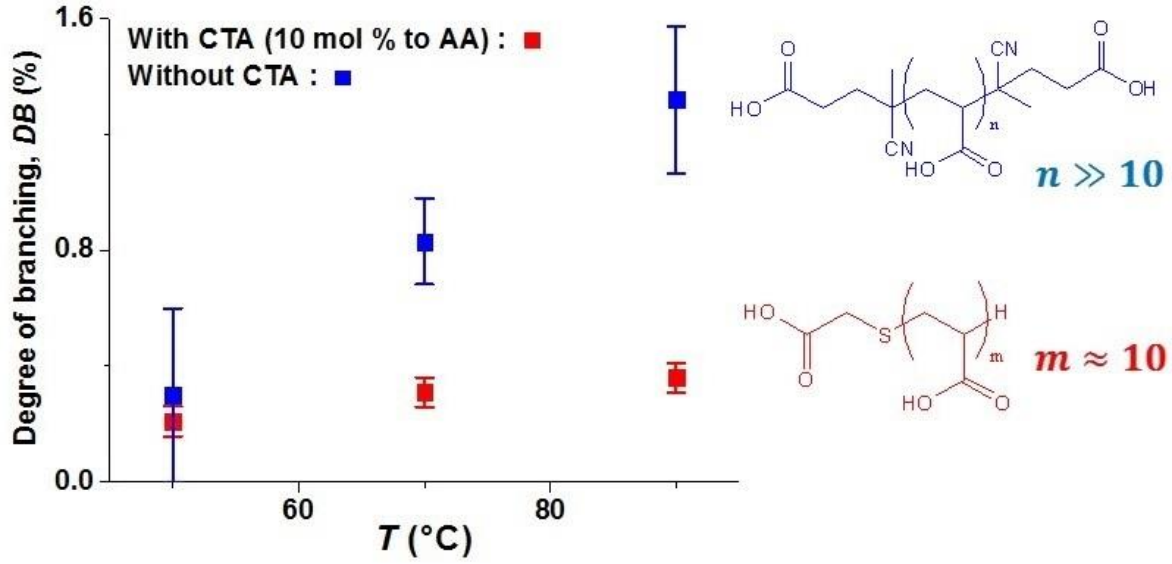

Effect of transfer agent, temperature and initial monomer concentration on branching in poly(acrylic acid): a study by ^{13}C NMR spectroscopy and capillary electrophoresis

Supplementary data

Jean-Baptiste Lena[a,b,c], Alexander K. Goroncy[a], Gregory T. Russell[a,*], Joel J. Thevarajah[b,c], Alison R. Maniego[b,c] , Patrice Castignolles[b,*], Marianne Gaborieau[b,c]

[a] *Department of Chemistry, University of Canterbury, Private Bag 4800, Christchurch, New Zealand*

[b] *Western Sydney University, Australian Centre for Research on Separation Science (ACROSS), School of Science and Health, Locked Bag 1797, Penrith NSW 2751, Australia*

[c] *Western Sydney University, Molecular Medicine Research Group, School of Science and Health, Locked Bag 1797, Penrith NSW 2751, Australia*

1. Synthesis of poly(acrylic acid)

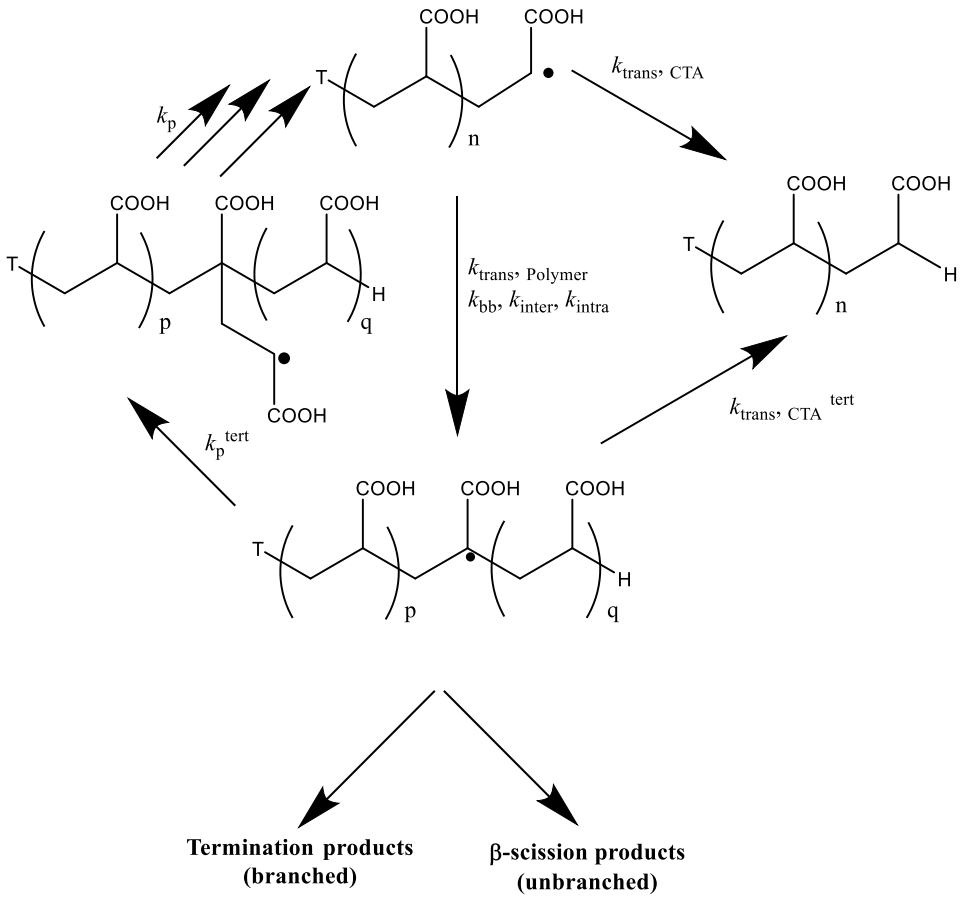

Figure S1: Reaction pathways for mid-chain radicals (MCRs) in the presence of chain transfer agent (CTA) (adapted from [1])

Table S1: Reaction times

Temperature	Reaction time	Half-time for decomposition of 4,4'-azobis(4-cyanovaleric acid) *
50 °C	24 h	96.6 h
70 °C	6 h	5.40 h
90 °C	1 h	24.9 mn

* Calculated using a frequency factor of 6.21×10^{15} s^{-1} and an activation energy of 132.9 kJ mol^{-1} [2]

2. Determination of the monomer conversion

Monomer conversion in acrylic acid polymerization is commonly determined in the literature using ^{1}H NMR spectroscopy[3, 4] and gravimetry[5-9] but also by HPLC[10], UV absorbance at 260 nm, Near-Infrared (NIR) spectroscopy[8, 11] (or NIR checked by ^{1}H NMR[12]) and calorimetry[13].

In the case of PAA synthesized at 50 °C with CTA and $[AA]_0$ = 2 M, the gravimetry indicated an average conversion of 66 % only, but with a standard deviation of 20 % (n=3). The low precision of this gravimetric measurement may add to a low accuracy because of the presence of both THF and water to evaporate in the gravimetry. The monomer conversion was thus also measured by solution-state ^{1}H NMR and the conversion was found to be high (Table S-2). The discrepancy between the values determined by gravimetry and ^{1}H NMR is large with values of 66 % (gravimetry, large error) and 98 % by ^{1}H NMR on the same sample. The large conversion observed by NMR spectroscopy was thus confirmed by a completely different method, namely free solution capillary electrophoresis (CE).

CE of pure acrylic acid monomer leads to 3 full resolved peaks (dashed line on figure S-2). The sodium acrylate is likely the peak at 2.5×10^{-8} m^2 V^{-1} s^{-1}. The peak at 3.30×10^{-8} m^2 V^{-1} s^{-1} is likely from poly(sodium acrylate) generated by autopolymerization. It is to be noted that the bottle of acrylic acid used for this experiment was different from the one used for the polymerization (it was provided by Aldrich and the purity was superior to 99%). The small peak at 2.05×10^{-8} m^2 V^{-1} s^{-1} could be either a dimer or an inhibitor. The preliminary study to determine the monomer conversion was performed with a fused-silica capillary of about 60 cm total length and with sodium borate at pH = 9.2 as buffer at a concentration close to 100 mmol L^{-1}. The conversion was determined as the ratio of the polymer peak area to the polymer, monomer and dimer peak areas. The UV absorption (Beer-Lambert) coefficient of the monomer is expected to be higher than the one of the carboxylate (chromophore) moiety of the polymer. The peak attributed to the dimer may be another species such as the inhibitor. For both these reasons, we expect these conversion values to be an underestimate of the monomer conversion. The monomer conversion determined by CE is higher than 88 % in the presence of thiol and consistent with the one determined by NMR spectroscopy. The monomer conversion is expected to be at least higher fo the polymerization in the absence of thiol since the rate of polymerization is generally observed to be higher in the absence of transfer agent.

Table S2: Monomer conversion determined by ^{1}H NMR spectroscopy

Polymer (PAA) synthesis conditions	Conversion by NMR (%)	*SNR* (residual monomer) NMR	*SD* (%) of the residual monomer in NMR	Conversion by CE (%)	SD (%) of the conversion by CE (%, n=3)
50 °C with a CTA and at $[AA]_0$ = 2M	98.0	38	0.04	99.3	0.2
50 °C without a CTA and at $[AA]_0$ = 2M	93.8	240	0.1		
70 °C with a CTA and at $[AA]_0$ = 2M	98.8	24	0.05	99.0	0.6
70 °C without a CTA and at $[AA]_0$ = 2M	97.4	58	0.05		
90 °C with a CTA and at $[AA]_0$ = 2M	>99.9 *			88.4	4.0
90 °C without a CTA and at $[AA]_0$ = 2M	97.6	61	0.05		
90 °C without a CTA and at $[AA]_0$ = 1M	99.9	5.2	0.03		
90 °C without a CTA and at $[AA]_0$ = 3M	98.9	25	0.04		

* no residual monomer detected.

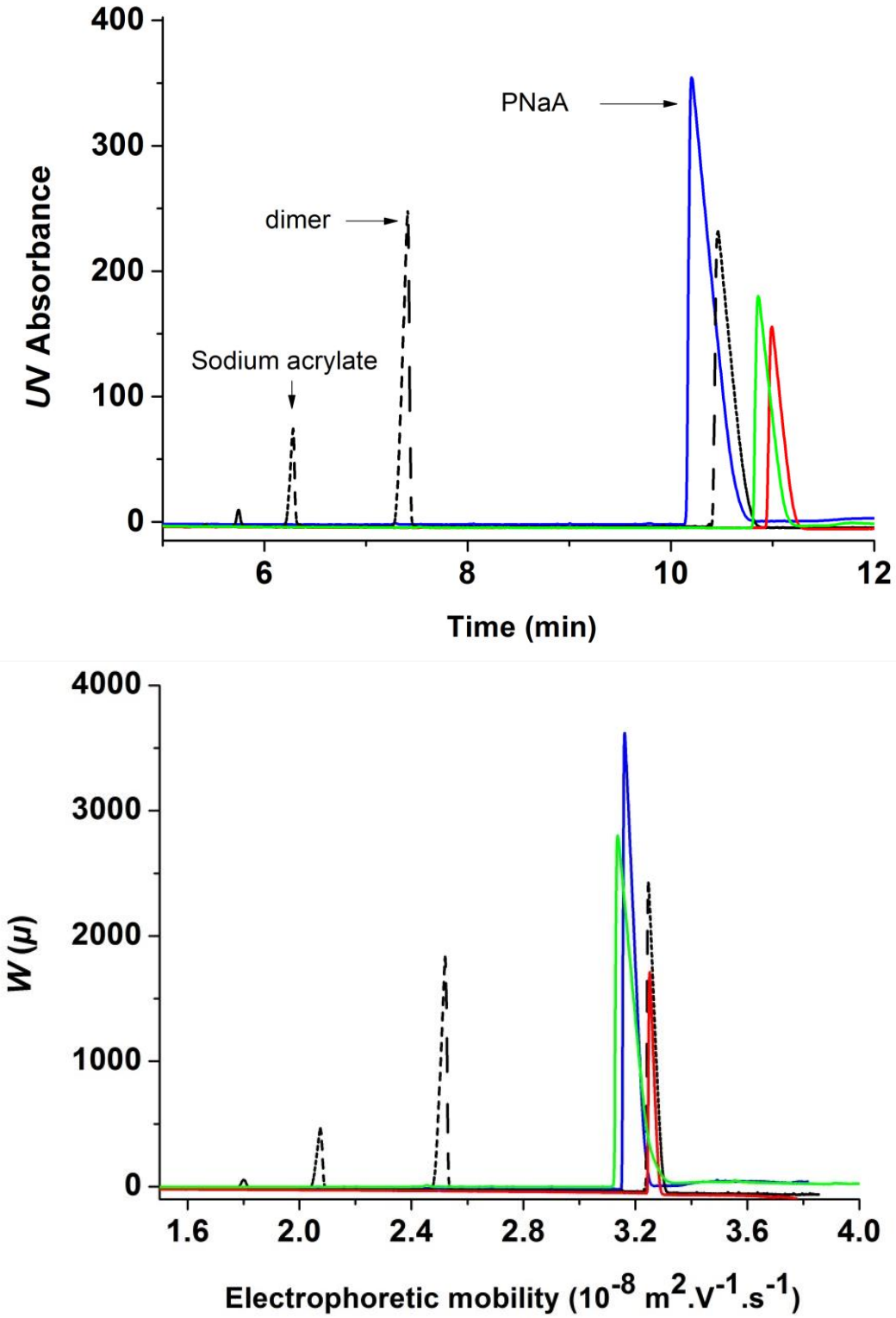

Figure S2: Separation of sodium acrylate and poly(sodium acrylate) by capillary electrophoresis (CE) shown as raw electropherogram (top) and distribution of electrophoretic mobility (bottom). Acrylic acid (black dashed line) was prepared at 2 g/L in 1 mM aqueous NaOH spiked with DMSO. PAAs synthesized at 50 °C, 70 °C and 90 °C with CTA (red, green and blue lines, respectively) were injected as crude medium diluted by a factor of 100 with water.

3. Mass spectrometry

M_{exp} is the experimental molar mass obtained for an adduct, M_{th} is the theoretical molar mass of the same adduct calculated with the mMass software, and h_{peak} is the peak height.

Table S2: Species detected by ESI-MS for PAA synthesized at 50 °C

Formula	M_{exp} (amu)	M_{th} (amu)	h_{peak} (arbitrary units)
$C_2H_3O_2S(C_3H_4O_2)_{15}H$ H^+	1173.3175	1173.3174	1067
$C_2H_3O_2S(C_3H_4O_2)_{15}H$ Na^+	1195.2949	1195.2994	298

Table S3: Species detected by ESI-MS for PAA synthesized at 70 °C

Formula	M_{exp} (amu)	M_{th} (amu)	h_{peak} (arbitrary units)
$C_2H_3O_2S(C_3H_4O_2)_7H$ H^+	1173.3048	1173.3174	1828
$C_2H_3O_2S(C_3H_4O_2)_7H$ Na^+	1195.2858	1195.2994	782
$C_2H_3O_2S(C_3H_4O_2)_{32}H$ 2 H^+	1199.3287	1199.3419	564
$C_2H_3O_2S(C_3H_4O_2)_{32}H$ Na^+ H^+	1210.3189	1210.3329	358
$C_2H_3O_2S(C_3H_4O_2)_{32}H$ 2 Na^+	1221.3129	1221.3239	281

Table S4: Species detected by ESI-MS for PAA synthesized at 90 °C

Formula	M_{exp} (amu)	M_{th} (amu)	h_{peak} (arbitrary units)
$C_2H_3O_2S(C_3H_4O_2)_7H$ H^+	1173.3038	1173.3174	4680
$C_2H_3O_2S(C_3H_4O_2)_7H$ NH_4^+	1190.3295	1190.3440	324
$C_2H_3O_2S(C_3H_4O_2)_7H$ Na^+	1195.2846	1195.2994	1754
$C_2H_3O_2S(C_3H_4O_2)_{32}H$ 2 H^+	1199.328	1199.3419	690
$C_2H_3O_2S(C_3H_4O_2)_{32}H$ Na^+ NH_4^+	1246.83	1218.8462	479
$C_2H_3O_2S(C_3H_4O_2)_{32}H$ 2 Na^+	1221.309	1221.3239	361

4. NMR spectroscopy

Concentration of PAA for NMR analyses and previous work for assessment of branching in PAA by ^{13}C NMR spectroscopy:

Table S5: [PAA] in D_2O for each ^{13}C NMR experiment

Samples	Concentration in D_2O
PAA synthesized at 50 °C with CTA at $[AA]_0$ = 2 M	750 mg mL^{-1}
PAA synthesized at 50 °C without CTA at $[AA]_0$ = 2 M	100 mg mL^{-1}
PAA synthesized at 70 °C with CTA at $[AA]_0$ = 2 M	750 mg mL^{-1}
PAA synthesized at 70 °C without CTA at $[AA]_0$ = 2 M	190 mg mL^{-1}
PAA synthesized at 90 °C with CTA at $[AA]_0$ = 2 M	750 mg mL^{-1}
PAA synthesized at 90 °C without CTA at $[AA]_0$ = 2 M	190 mg mL^{-1}
PAA synthesized at 90 °C without CTA at $[AA]_0$ = 1 M	190 mg mL^{-1}
PAA synthesized at 90 °C without CTA at $[AA]_0$ = 3 M	190 mg mL^{-1}
PAA supplied by Sigma-Aldrich	27 mg mL^{-1}

Table S6: Conditions for ^{13}C NMR analyses of branching in PAA and PNaA in the literature.

Sample	Solvent	Concentration	Temperature	Repetition delay	Pulse angle	Larmor frequency	Type of study	Ref.
Linear PNaA	D_2O	150 g L^{-1}	RT*	20 s	90°	75 MHz	Detection of branching	[14]
Hyperbranched PNaA	1,4-Dioxane-d_8	50 g L^{-1}	RT	20 s	90°	75 MHz	Detection of branching	[14]
3-arm star PNaA (synthesized by NMP, trifonctional initiator)	D_2O with 428 nM NaOH	50 g L^{-1}	RT	20 s	90°	75 MHz	Detection of branching	[14]
PNaAs synthesized by RAFT	D_2O	30 % (w/w)	60 °C	4.5 s	70°	100.6 MHz	Quantification of branching	[10]
PNaAs synthesized by NMP	D_2O	Not given	RT	20 s	20°	125.7 MHz	Quantification of branching	[15]
PAAs produced by batch radical polymerization	D_2O	Not given	Not given	Not given	Not given	Not given	Quantification of branching	[12]

* RT stands for room temperature

NMR of PAA and signal assignment:

All PAAs were analyzed by ^{1}H and ^{13}C NMR spectroscopy. All thiol and non thiol-containing PAAs had similar spectra. Examples of ^{1}H and ^{13}C NMR spectra are given in Figures S3 to S6.

Table S7: Signal assignment for ^{1}H NMR spectra of PAA in D_2O at 26 °C

δ (ppm) for thiol-containing PAA	**δ (ppm) for non thiol-containing PAA**	**δ (ppm) Literature [14] (analyses done in D_2O with NaOH at RT)**	**δ (ppm) Literature [10] (analyses done in D_2O at 60 °C)**	**δ (ppm) Literature [16] (analyses done in dioxane-d_8 at RT)**	**δ (ppm) ChemNMR calculations and solvent table[17] in the case of residual water**	**Assignment**
1.65-1.95	1.65-1.95	1.3-1.8	1.3-1.8	1.0-1.8	1.75	C**H$_2$** (main chain)
2.3-2.5	2.3-2.5	2-2.3	1.9-2.3	1.8-2.3	2.35	C**H** (main chain)
2.75		-	-	2.60	2.33	CH_2-C**H$_2$**-COOH (end group)
2.88		-	-	2.87	1.79	C**H$_2$**-CH_2-COOH (end group)
3.4	-	-	-	-	3.38	S-C**H$_2$**-COOH (end group)
4.76	4.7	-	4.7	-	4.79	Residual solvent
6	6	5.8-5.9	-	-	5.75	monomer (H in cis to COOH)
6.2	6.2	5.9-6	-	-	6.22	monomer (H on same C as COOH)
6.4	6.4	6.7	-	-	6.50	monomer (H in trans to COOH)

Table S8: Signal assignment for ^{13}C NMR spectra of PAA in D_2O at 49 °C

δ (ppm) for thiol-containing PAA	δ (ppm) for non thiol-containing PAA	δ (ppm) Literature [14] (analyses done in D_2O with NaOH at RT)	δ (ppm) Literature [10] (analyses done in D_2O at 60 °C)	δ (ppm) Literature [16] (analyses done in dioxane-d_8 at RT)	δ (ppm) ChemNMR calculations	assignment
27.5	-	-	-	-	27.4, 29.6	CH_2-**C**H_2-COOH, **C**H_2-CH_2-COOH(end group)
31.8	-	-	-	-	30.9	**C**H_2-S-CH_2-COOH (end-group)
34-36	34-36	36-39	30.5-33	35-40	26-27.5	CH_2 (main chain)
36.5-37.5	36-37	-	38-39	-	-	CH_2 adjacent to a branch
39.6-40.4	39.8-40.8	-	41.8-43.4	-	-	CH adjacent to a branch
41-42.5	41-43	45-47	43.6-48	44.5-48.5	40-41	CH (main chain)
43	-	-	-	-	43.6	COOH-CH_2-S-CH_2-**C**H
44	-	-	-	-	44.5	COOH-**C**H_2-S (end group)
48.2	48.3	50.4	48.5-50	-	-	quaternary carbon (branching point)
128.3	128.3	127	-	-	127.5	HC(sp^2) unreacted monomer
133.4	133.4	135	-	-	134.1	H_2C(sp^2) unreacted monomer
170.5	170.5	-	-	-	170.4	COOH unreacted monomer
174.9	-	-	-	-	174.6	S-CH_2-**C**OOH (end group)
176.5	-	-	-	-	-	not identified
178	-	-	-	-	178.3	**C**OOH-CH-CH_2-S
179-179.5	179-179.5	-	-	183-187	182.9	**C**OOH main chain

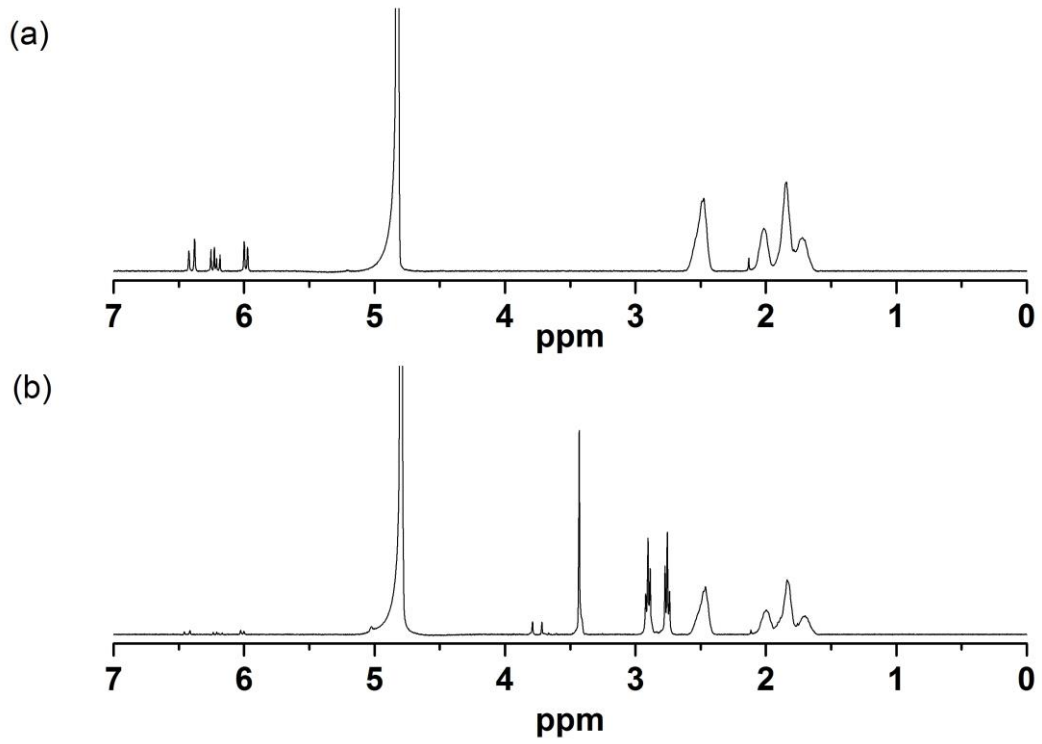

Figure S3: Full ^{1}H solution-state NMR spectra in D_2O at 26 °C of PAA synthesized at 50 °C (a) without CTA and (b) with CTA.

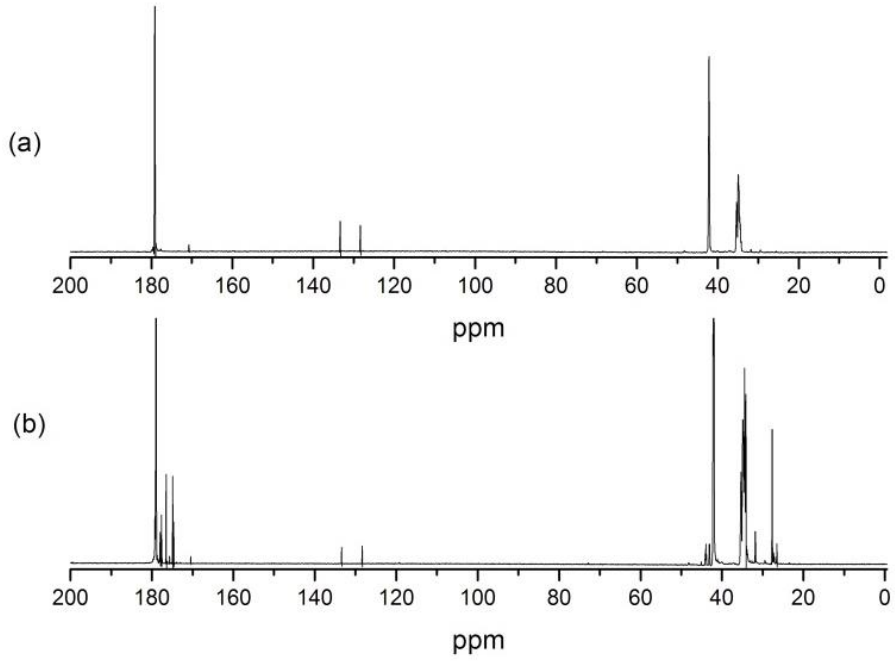

Figure S4: Full ^{13}C solution-state NMR spectra in D_2O at 49 °C of PAA synthesized at 90 °C (a) without CTA and (b) with CTA.

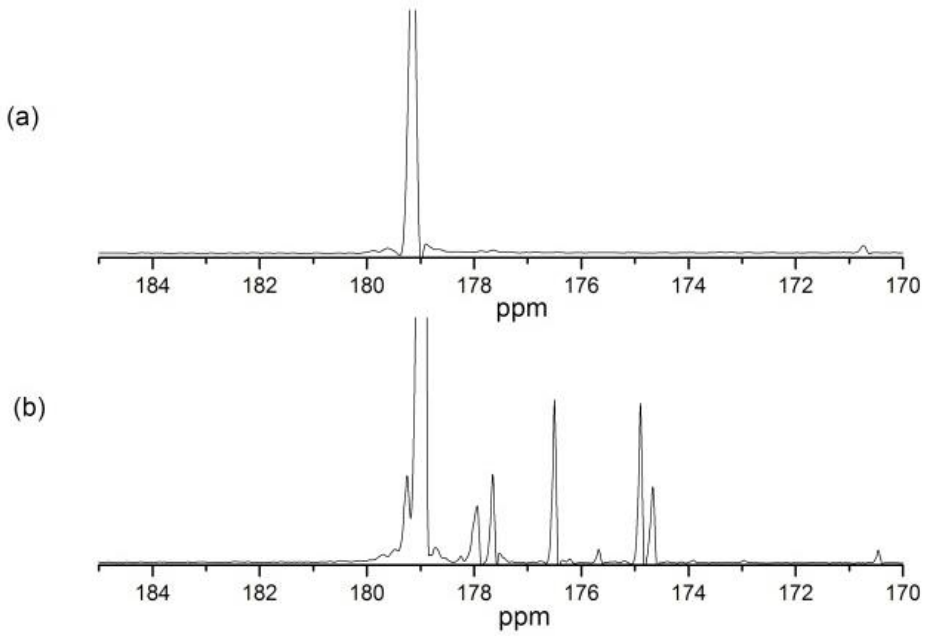

Figure S5: Partial ^{13}C solution-state NMR spectra in D_2O at 49 °C of PAA synthesized at 90 °C (a) without CTA and (b) with CTA.

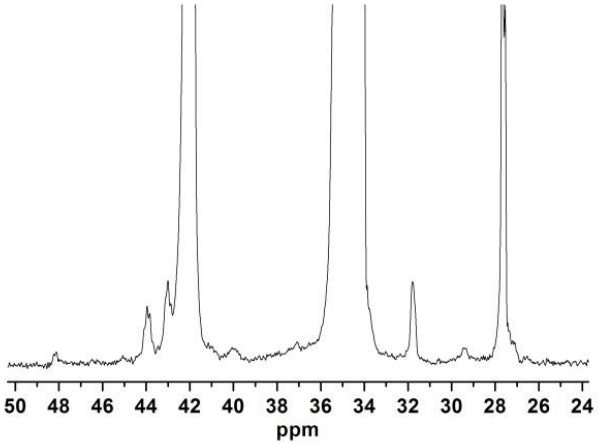

Figure S6: Partial ^{13}C NMR spectrum of PAA synthesized at 70 °C with CTA, analyzed at 750 g L^{-1} in D_2O. The signals of C adjacent to the sulfur and of main-chain CH are overlapping.

Two-dimensional NMR of PAA

In order to identify the signals and to check if some signals of impurities were overlapping with the quantified signals, the COSY and HSQC NMR analyses of PAA were carried out (see Figure S7).

It was shown that nothing is overlapping with the main-chain CH signal (42 ppm) and the branching signal (48 ppm).

COSY and HSQC spectra were acquired at 26 °C in D_2O on an Agilent 400 MR with Varian 7600-AS auto-sampler, equipped with OneNMR probe and variable temperature capabilities, operating at a Larmor frequency of 399.84 MHz for ^{1}H and 100.55 MHz for ^{13}C. 2D HSQC (^{1}H, ^{13}C) spectra were acquired with (1024, 1024) data points, 32 scans, (6,404.0 Hz, 20,090.97 Hz) spectral width, (0.1501 s, 0.0048 s) acquisition time, 4.5 s relaxation delay, and with the pulse program bsHSQCAD. 2D COSY (^{1}H, ^{1}H) spectra were acquired with (1150, 128) data points, 1 scan, (7,662.04 Hz, 7,608.80 Hz) spectral width, (0.1501 s, 0.0048 s) acquisition time, 1.0 s relaxation delay, and with the pulse program gCOSY.

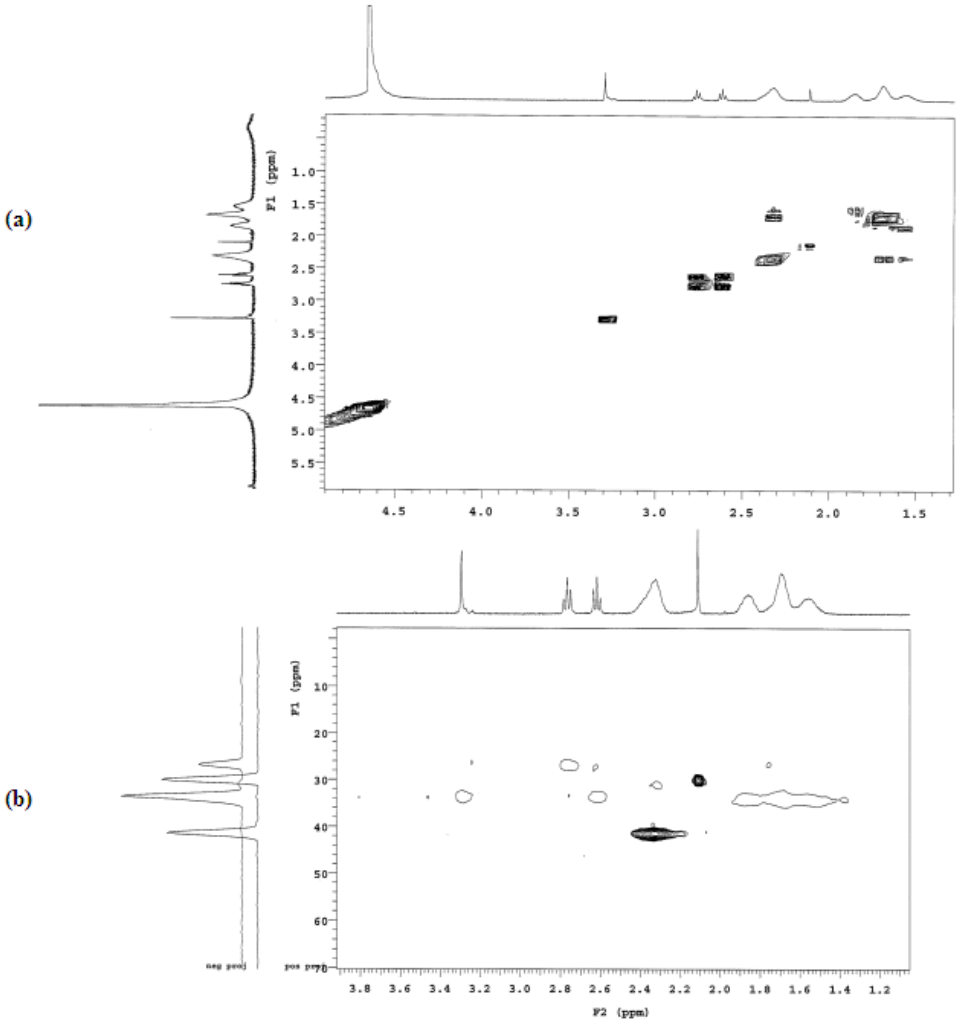

Figure S7: Two-dimensional NMR of CTA-containing PAA synthesized at 70 °C, analyzed in D_2O: (a) COSY; (b) HSQC, white shapes represent CH_2 and black shapes represent CH and CH_3.

Estimation of the longitudinal relaxation time

In order to obtain quantitative results, it is necessary to have an estimation of the longitudinal relaxation time, T_1, of each signal that will be quantified.

The most common experiment used to determine T_1 is a so-called inversion recovery experiment [18].

This experiment consists of a 2-pulse sequence. In a first step, the spin population is inverted through the application of a 180° pulse. The magnetization vector will first shrink back toward the X-Y plane and then make a full recovery along the Z-axis at a rate dictated by the relaxation time T_1. As the magnetization along the Z-axis is not observable, the vector will be placed back in the X-Y plane with a 90° pulse after a suitable waiting time τ.

For a short τ, the magnetization vector will be located along the negative Y axis, and a negative signal will be observed. For a long τ, the magnetization vector will be recovered and a positive signal will be observed.

The intensity of the detected magnetization M_τ follows Eq. (S1):

$$M_\tau = M_0 \left(1 - 2e^{-\tau/T_1}\right) \quad \text{(S1)}$$

So the experiment is repeated for several values of τ, and when extinction of the signal is observed, the waiting time corresponds to $\tau_{\text{null}} = T_1\, ln2$.

The branching was observable with a *SNR* > 5 only after 53 h (except for the PAA synthesized at 50 °C without CTA). So, it would unpractical and very expensive to perform a full inversion recovery experiment with many values of τ. However it is possible to check if the repetition time between 2 pulses (acquisition time + relaxation delay) used when the branching was detected is greater than $5T_1$. In that case, these parameters are valid for quantitative NMR spectroscopy analysis.

The spectra were recorded with 10 s relaxation delay and 1.311 s acquisition time. So, if 11.311 s > $5T_1$, i.e., if τ_{null} < 1.568 s for C_q and main-chain CH signals, the analysis is quantitative. An inversion recovery experiment with τ = 1.568 s was completed. It was found that the C_q signal and the signals of the main chain CH and the CH adjacent to a branch are positive (see Figure S8). Consequently, the condition for quantitative analysis is fulfilled.

Another experiment was performed to check if a relaxation delay of 6.5 s with an acquisition time of 1.311 s was enough to be quantitative (which means if τ_{null} < 1.082 s). However, Figure S9 shows that the quaternary carbon signal is in its extinction zone (not observable in the spectrum). It may be exactly absent, slightly positive, or slightly negative (below the noise level). Thus it is unsure if a ^{13}C NMR signal recorded with the corresponding repetition time is quantitative.

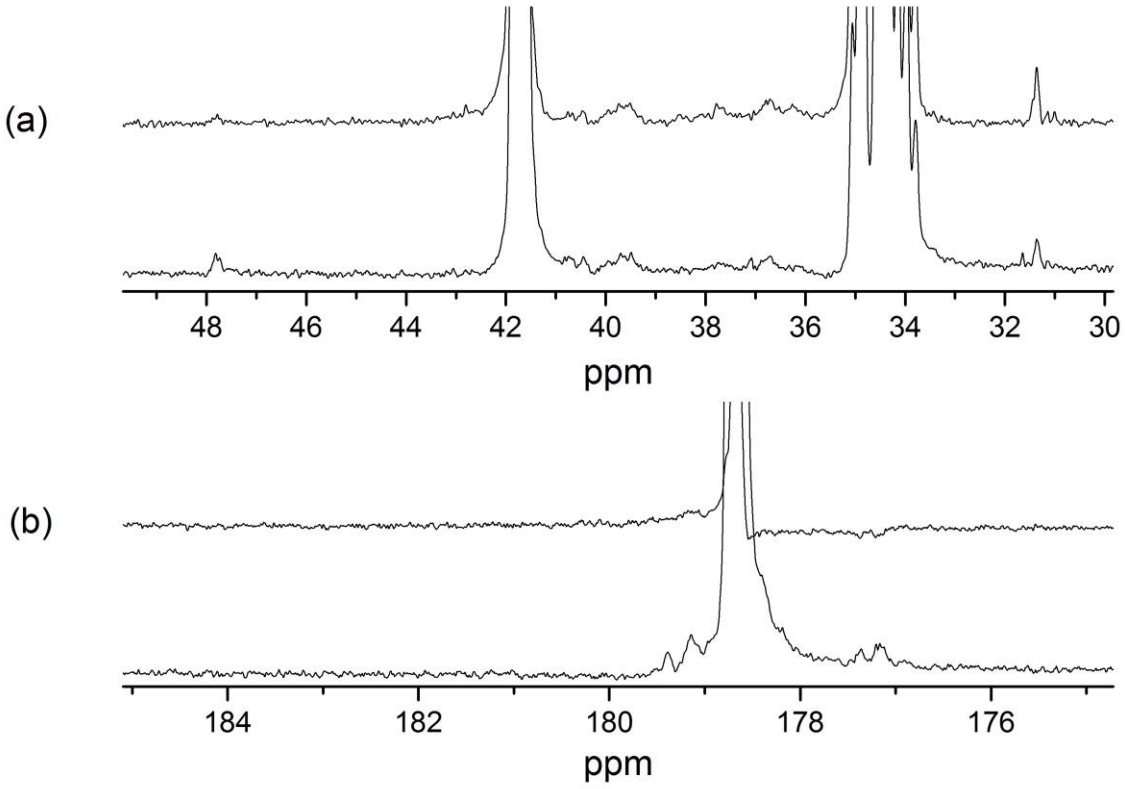

Figure S8: Partial ^{13}C NMR spectra of PAA synthesized at 70 °C without CTA: top – obtained from an inversion recovery experiment with τ = 1.568 s; bottom – regular conditions.

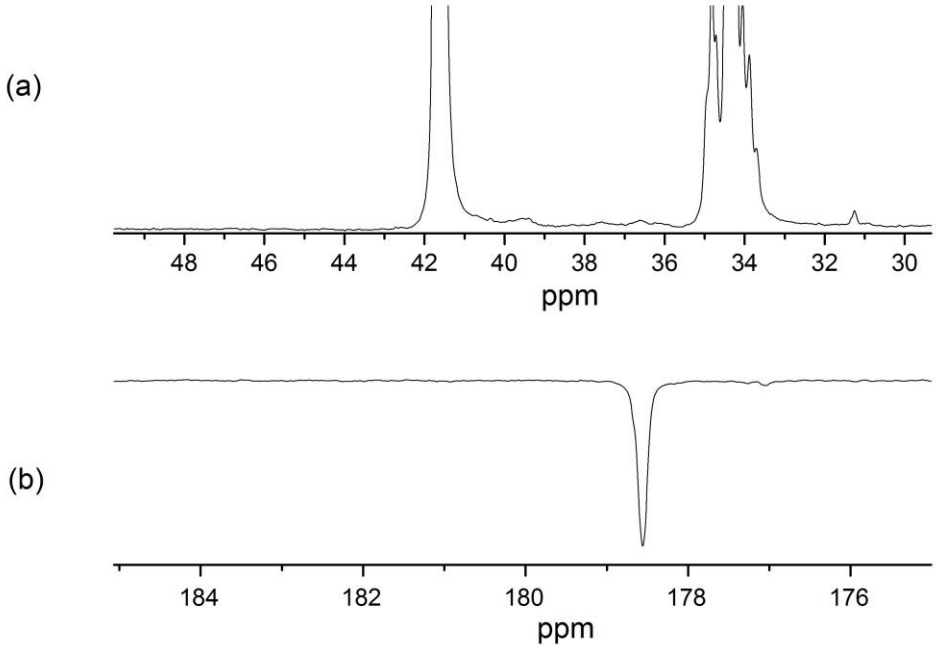

Figure S9: Partial ^{13}C NMR spectrum of PAA synthesized at 70 °C without CTA obtained from an inversion recovery experiment with τ = 1.082 s.

Table S9: overestimated values of the longitudinal relaxation time T_1 measured for the signals of interest for DB quantification of PAA in different conditions.

Samples	*Conditions of NMR analyses*	*T_1 of signals of interest for DB quantification*
PAAs synthesized in this work	D_2O, 49 °C	1.56 s < T_1 < 2.26 s for the C_q signal T_1 < 1.56 s for CH and CH_2 signals (main chain) 1.56 s < T_1 < 2.26 s for COOH signal (main chain)
PAA from Sigma	D_2O/NaOD, RT	T_1 < 1.2 s the C_q signal, T_1 < 1.2 s for the CH and CH_2 signals (main chain) T_1 < 1.2 s for COOH signal (main chain)

Degree of branching (*DB*): equations and results

Table S10: *DB* of PAAs calculated with different equations and its relative standard deviation (*RSD*) based on the signal to noise ratio (*SNR*) of the C_q (calculated using Eq. (5) of the main text).

PAA synthesis	*DB (%) from Eq. (1) or Eq. (S3)**	*DB (%) from Eq. (3) (underestimate)*	*DB (%) from Eq. (2) (overestimate)*	*DB (%) from Eq. (4)*	*SNR*	*RSD (%)*
90 °C with CTA and at $[AA]_0$ = 2 M	–	0.36	0.37	0.37	9.22	13.9
70 °C with CTA and at $[AA]_0$ = 2 M	–	0.31	0.33	0.32	8.16	16.4
50 °C with CTA and at $[AA]_0$ = 2 M	–	0.21	0.25	0.23	5.85	24.8
90 °C without CTA and at $[AA]_0$ = 2 M	1.32	–	–	1.28	7.15	19.2
70 °C without CTA and at $[AA]_0$ = 2 M	0.83	–	–	0.83	7.55	17.9
50 °C without CTA and at $[AA]_0$ = 2 M*	Below 0.61*	–	–	–	2.62	–
90 °C without CTA and at $[AA]_0$ = 1 M	1.36	–	–	1.37	9.28	13.8
90 °C without CTA and at $[AA]_0$ = 3 M	1.16	–	–	1.17	6.94	20.0
Sigma-Aldrich	–	–	–	1.13	16.75	6.45

* For the PAA synthesized at 50 °C without CTA, the *SNR* was below 3, which means below the limit of detection (LOD). It is thus not possible to confirm whether this polymer is branched or not. To estimate a maximum possible degree of branching, the *SNR* of the main chain CH signal and the one of the C_q signal were compared as follows (Eq. S3).

$$DB(\%) = \frac{100 \cdot I(\mathrm{C}_q)}{I(\mathrm{C}_q)+I(\mathrm{CH})} = \frac{100}{1+\frac{I(\mathrm{CH})}{I(\mathrm{C}_q)}} \quad \text{(S2)}$$

Figure S10 shows that $SNR(\mathrm{CH}) / SNR(\mathrm{C}_q) \approx I(\mathrm{CH}) / I(\mathrm{C}_q)$, meaning that equation (S3) provides an estimation for a maximum potential *DB:*

$$DB_{max}\ (\%) = \frac{100}{1+\frac{SNR(\mathrm{CH})}{SNR\ (\mathrm{C}_q)}} \quad \text{(S3)}$$

This equation was used for this one particular case.

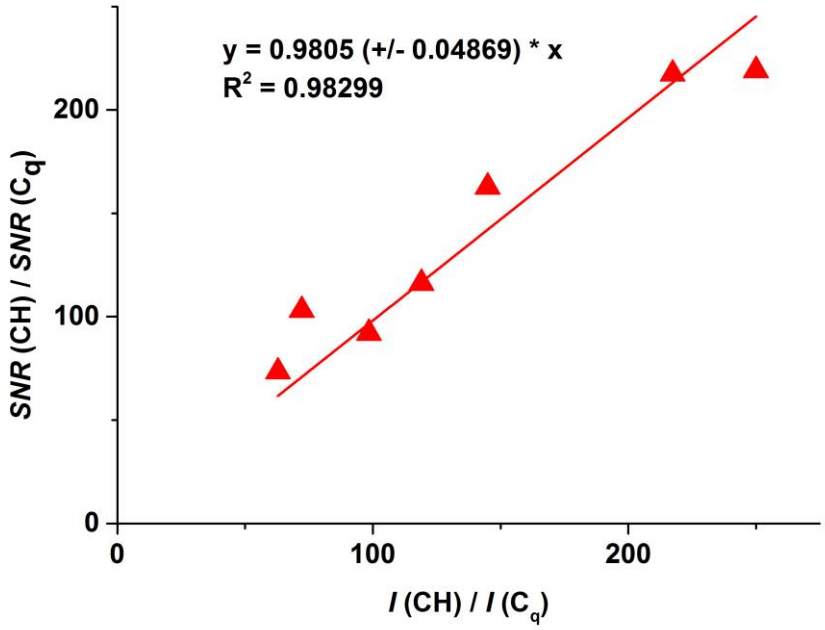

Figure S10: Ratio of the *SNR*s of the backbone CH and C_q signals as a function of the ratio of their integrals for the experiments of this work.

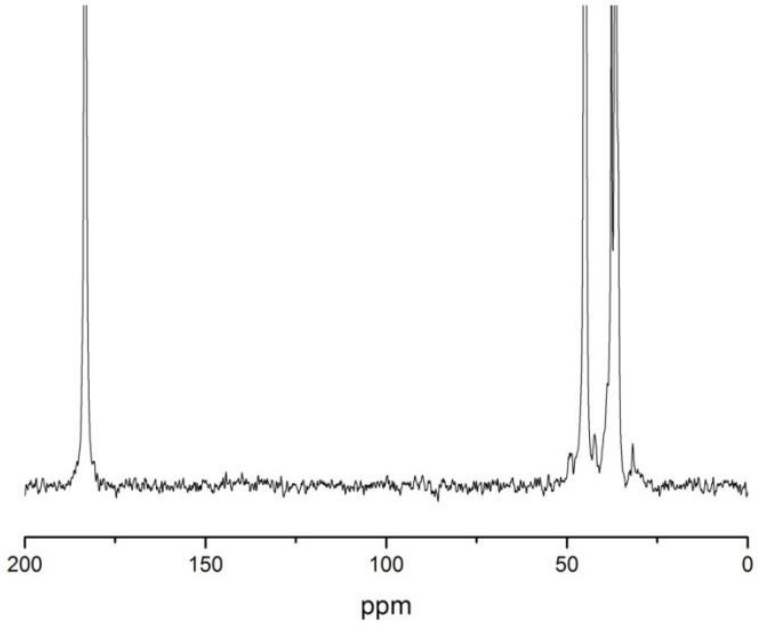

Figure S11: ^{13}C NMR spectrum of PAA provided by Sigma-Aldrich, analyzed at 27 g L^{-1} in D_2O (with 1 mol eq. of NaOD and 0.5 mol eq. of DCl) at room temperature.

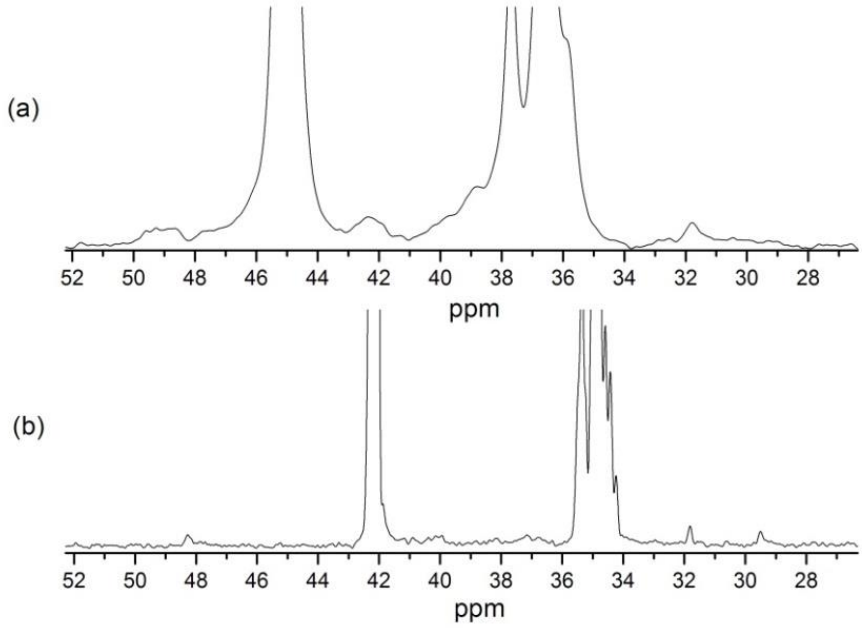

Figure S12: Partial ^{13}C NMR spectra of (a) PAA supplied by Sigma-Aldrich, analyzed at room temperature at 27 g L^{-1} in D_2O (with 1 mol eq. of NaOD and 0.5 mol eq. of DCl) with 27,411 scans, and (b) PAA synthesized at 90 °C without CTA, analyzed at 190 g L^{-1} in D_2O at 49 °C with 17,500 scans.

Probing the dissolution of PAA in D_2O:

Dissolution of analytes can be analyzed by NMR spectroscopy [19].

$$Normalized\ PNR = \frac{PNR}{[analyte]\sqrt{number\ of\ scans}} \quad \text{(S4)}$$

The noise was measured in 2 steps. First, the *SNR* was measured using the ACD/Lab software and then, the height of the signals was measured with the Origin 9.0 software. The peak area was also measured with the Origin 9.0 software by integration of the signal.

The uncertainty of the normalized *PNR* was calculated based on the uncertainty of the concentration of analyte neglecting the error on the number of scans and the peak area (Eq. S5). The error on the mass was based on the last digit appearing on the scale (mg) and the error on the measured volume was calculated by weighting 5 times 1 mL of MilliQ water taken with 5 different 1 mL plastic syringes ($SD_{1\ mL\ syringes}$ = 0.016936 mL). In the case of the thiol-containing PAA synthesized at 70 °C, there is also an uncertainty on the peak area of main chain CH and C_{thiol} signals are overlapping.

$$Uncertainty\ (normalized\ PNR) = |Normalized\ PNR_{max} - Normalized\ PNR_{min}| \quad \text{(S5)}$$

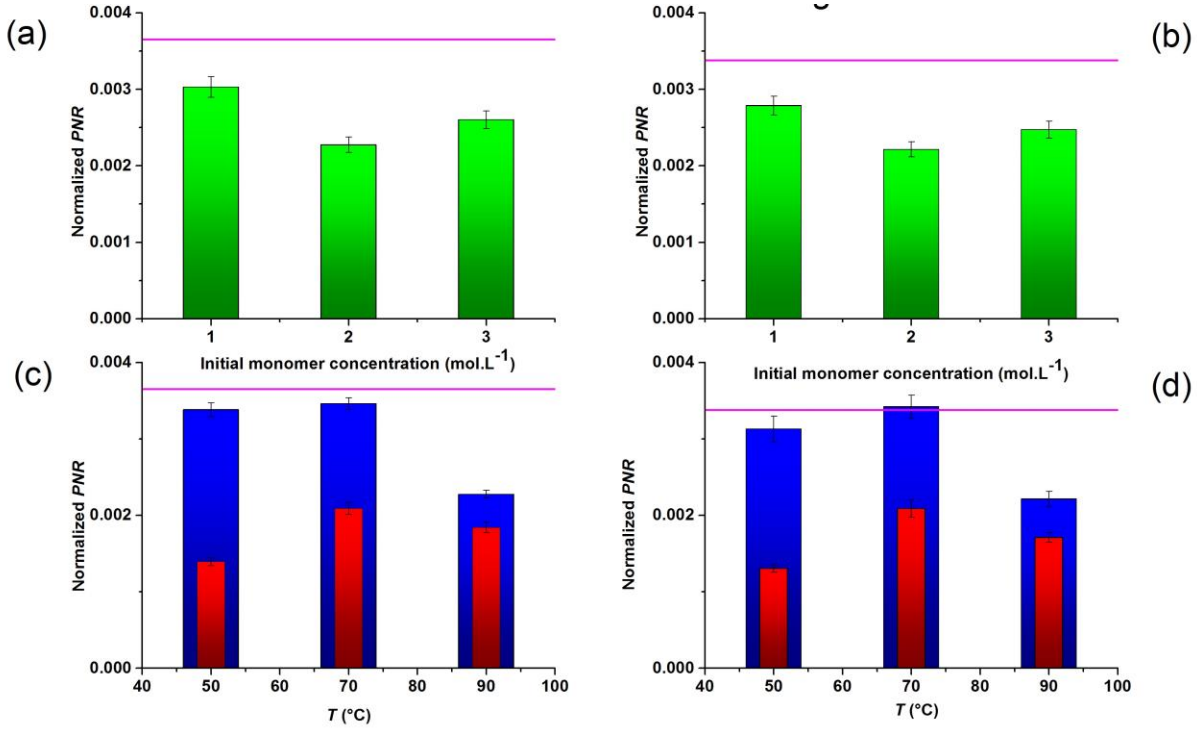

Figure S13: Normalized *PNR* of the different PAAs synthesized by conventional radical polymerization. Green bars represents the PAAs synthesized at 90 °C without CTA at different initial minomer concentrations, red and blue bars represent the PAAs synthesized at $[AA]_0$=2 M at different temperatures, with and without CTA, respectively. Graphs a and c represents the results obtained with the backbone COOH signal, b and d graphs represents the results obtained with the backbone CH signal. Magenta lines represent the *PNR* values obtained for the linear PNaA.

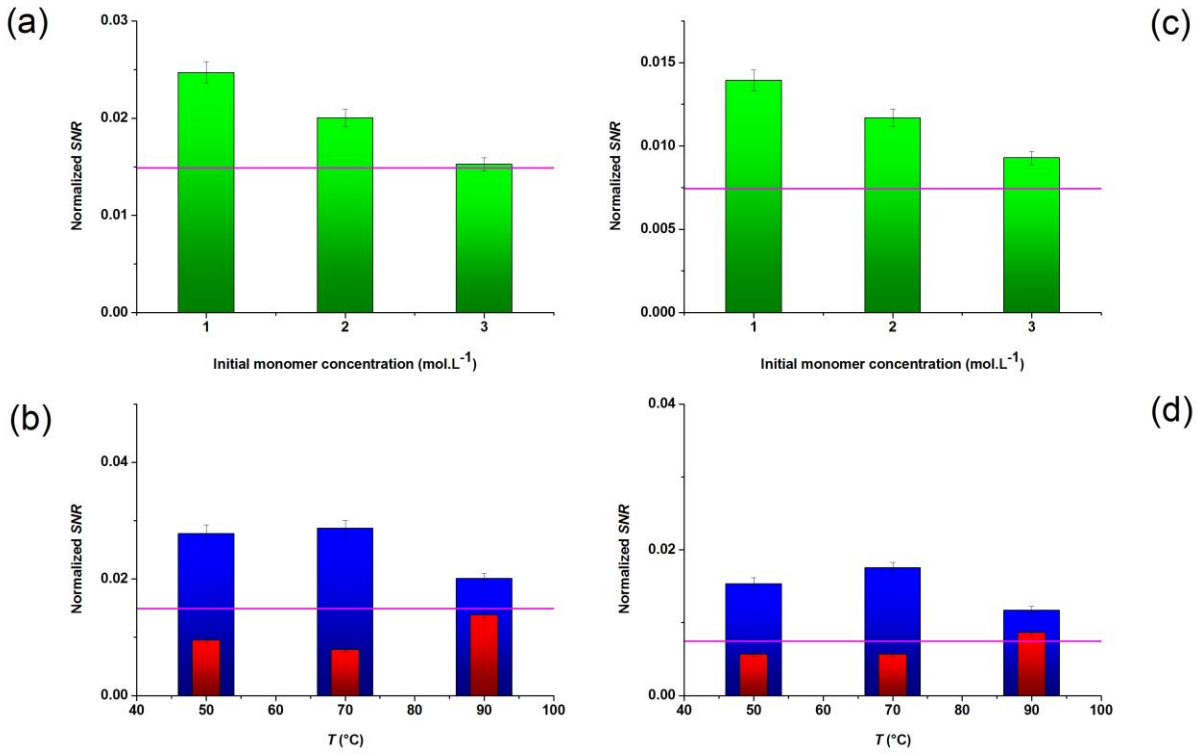

Figure S14: Normalized *SNR* of the different PAAs synthesized by conventional radical polymerization. Green bars represents the PAAs synthesized at 90 °C without CTA at different initial minomer concentrations, red and blue bars represent the PAAs synthesized at $[AA]_0$=2 M at different temperatures, with and without CTA, respectively. Graphs a and b represents the results obtained with the backbone COOH signal, c and d graphs represents the results obtained with the backbone CH signal. Magenta lines represent the *SNR* values obtained for the linear PNaA.

Effect of the contamination of the deuterium oxide:

A ^{1}H NMR analysis of the D_2O used to run the different analyses showed that this solvent has been contaminated with PAA (see Figure S15). In order to test the effect of the contamination on the study, a ^{13}C NMR analysis was run in same conditions as the quantitative analyses of PAA. Figure S16 shows that the contamination has a negligible impact on a regular spectrum. On the ^{13}C NMR spectrum of the contaminated D_2O, the main chain CH and main chain COOH signals have respectively *SNR* around 4 and 6, which is less than 1 % of the *SNR* of the same signals on regular spectra. So, the error potentially induced by the contamination on the *DB* is much lower than the calculated error bar of *DB*.

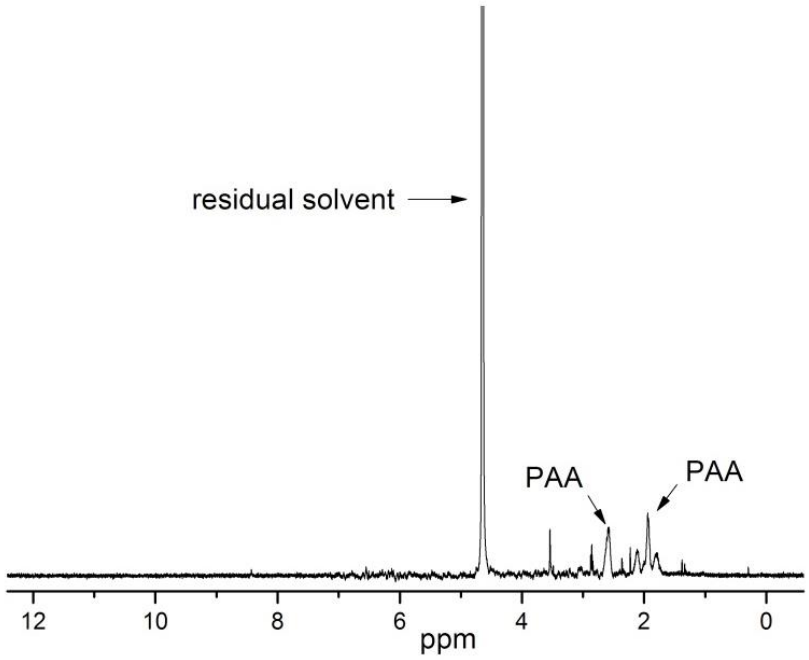

Figure S15: ^{1}H NMR spectrum of the contaminated D_2O

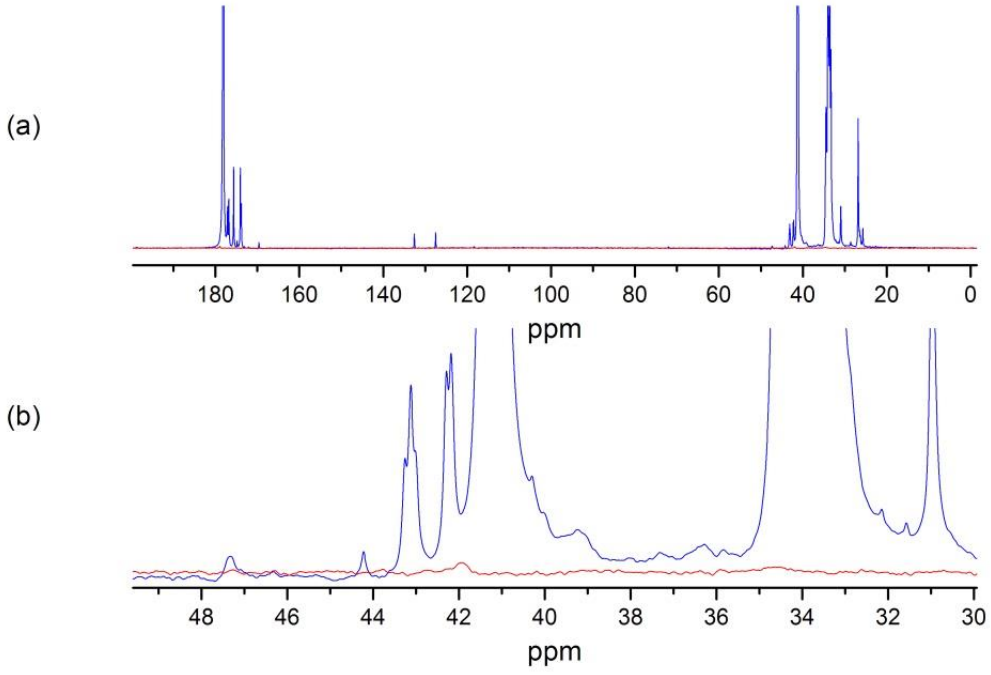

Figure S16: full (a) and partial (b) ^{13}C NMR spectra of PAA synthesized at 90 °C with thiol and $[AA]_0$=2 M (blue line) and of the contaminated D_2O (red line)

5. Kinetics of polymerization: Backbiting rate coefficients and degree of branching

Parameters used for the linear fits:

The values of the backbiting rate coefficients were estimated using equation (6) as well as the values of the propagation rate coefficient estimated from equation (S6). The final monomer conversion $[M]_e$ was calculated based on the monomer conversion estimated using CE for the polymer synthesized in the presence of CTA and using ^{1}H NMR spectroscopy for the polymer synthesized in the absence of CTA.

$$k_p(L.mol^{-1}.s^{-1}) = 3.2\ 10^7 e^{-\frac{1564}{T}}(0.11 + (1 - 0.11)e^{-3w'_{AA}}) \quad (S6)$$

In Eq. (S6), w'_{AA} is the wt. fraction of AA solution on a polymer-free basis. The average value of w'_{AA} over the polymerization process was used in order to calculate k_p.

Arrhenius equation:

$$\ln\ (k) = \ln(A) - \frac{E_A}{RT} \quad (S7)$$

Where k is the kinetic rate coefficient, A is the frequency factor (same unit as k), E_A is the activation energy (J.mol^{-1}), R is the ideal gas constant (J.K^{-1}.mol^{-1}), T is the temperature (K).

The slope and intercepts were calculated with the Origin 9.0 software.

$$k_{bb}\ (s^{-1}) = 9.94\ \times\ 10^8\ (s^{-1})\ e^{-\frac{4576}{T/K}} \quad (S8)$$

$$RSD\ (\ln k_{bb}) = \frac{RSD\ (DB)}{k_{bb}} \quad (S9)$$

Table S11: Linear fit parameters for the different Arrhenius plots of k_{bb}, where the slope refers to the activation energy and the intercept to the ln (A) where A is the frequency factor.

	k_{bb} (s^{-1}) from this study in the absence of CTA	**k_{bb} (s^{-1}) from this study in the absence of CTA excluding the polymerization at 90 °C and 1 M monomer**	**k_{bb} (s^{-1}) from this study in the presence of CTA**	**k_{bb} (s^{-1}) of Wittenberg *et al*. study [8, 12]**
slope (-Ea/R (J.mol^{-1}))	-3737	-5066	-4777	-4576
Standard error (slope)	1933	244	86	
Intercept (ln (A (s^{-1}))	17.8	21.8	20.1	20.7
Standard error (intercept)	5.5	0.7	2.4	
Correlation coefficient R^2	0.56	0.996	0.97	

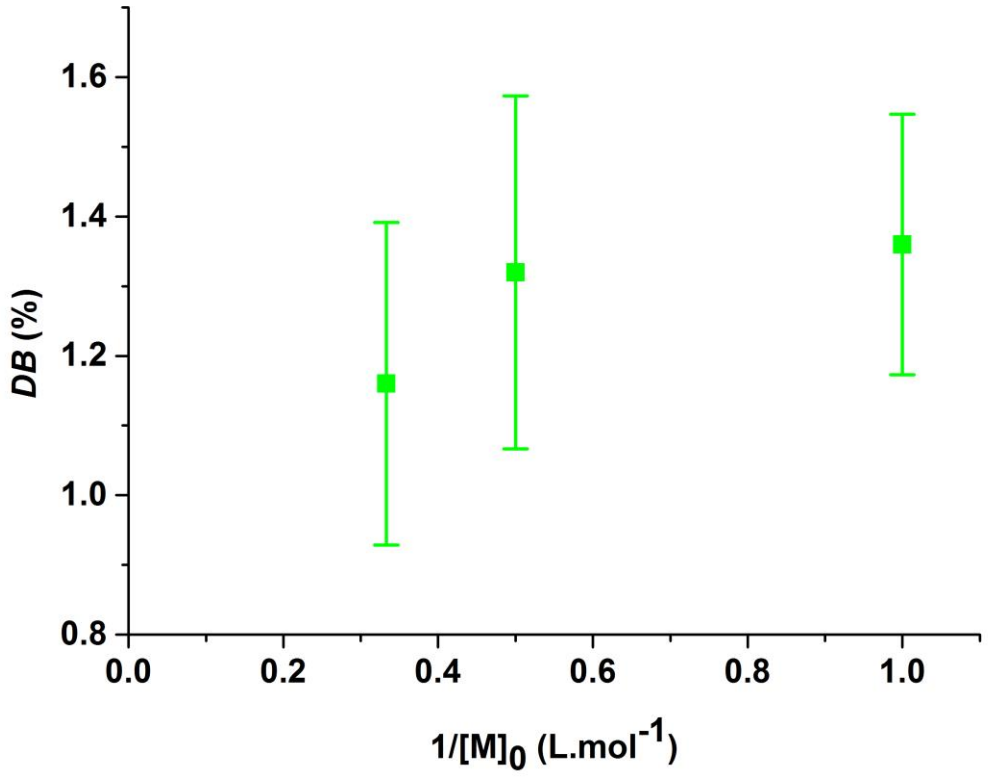

Figure S17: Average *DB* as a function of the inverse of the initial monomer concentration, where all experiments were at 90 °C and without CTA.

6. Capillary electrophoresis

Determination of the optimal injection concentrations

Preliminaries studies to determine the optimal injection concentrations were performed with a fused-silica capillary of about 60 cm total length and with sodium borate as buffer at a concentration close to 100 mmol.L^{-1}. For each sample, the concentrations of PAA and NaOH decreased by the same factor for their initial values through the sample dilution with water.

Table S12: Concentrations of injected PAAs without overloading

PAA sample synthesis	Concentration (g.L^{-1}) at which no overloading occurs	Concentration of NaOH (mmol.L^{-1})
50 °C with CTA, $[AA]_0$ = 2 M	6.67	10.0
50 °C without CTA, $[AA]_0$ = 2 M	0.208	0.313
70 °C with CTA, $[AA]_0$ = 2 M	1.67	2.50
70 °C without CTA, $[AA]_0$ = 2 M	0.833	1.25
90 °C with CTA, $[AA]_0$ = 2 M	1.67	2.50
90 °C without CTA, $[AA]_0$ = 1 M	0.833	1.25
90 °C without CTA, $[AA]_0$ = 2 M	0.833	1.25
90 °C without CTA, $[AA]_0$ = 3 M	0.417	0.625

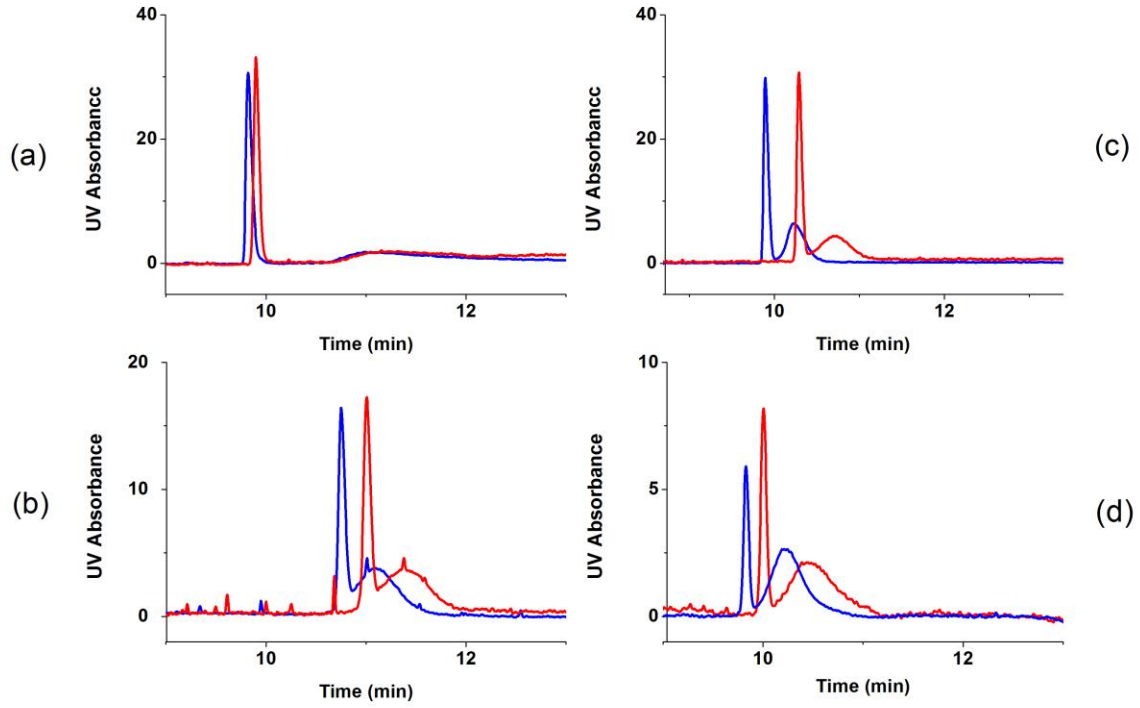

Figure S18: PAA synthesized at (a) 90 °C with CTA and $[AA]_0$ = 2 mol L^{-1}, (b) 90 °C without CTA and $[AA]_0$=1 mol L^{-1}, (c) 90 °C without CTA and $[AA]_0$ = 2 mol L^{-1}, (d) 90 °C without CTA and $[AA]_0$=3 mol L^{-1} . In all raw electropherograms, all PAA are injected at 2 different concentrations: the concentration at which no overloading occurs (see table S11) (blue line) and half of it (red line).

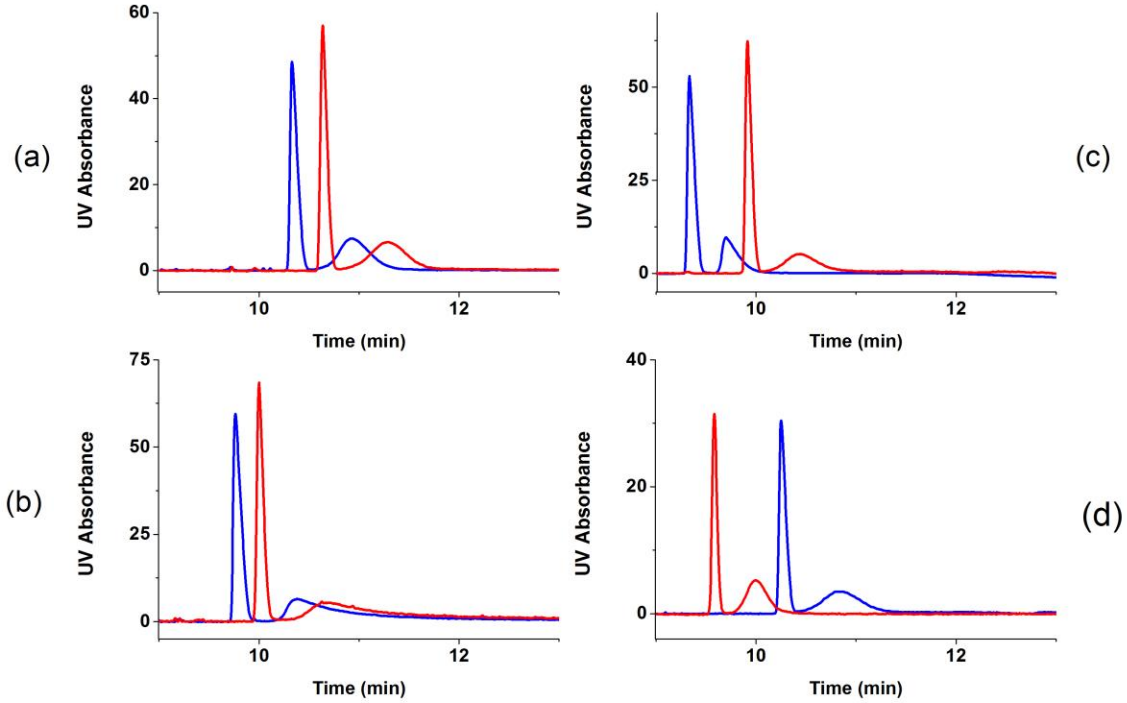

Figure S19: PAA synthesized at (a) 50 °C with CTA and $[AA]_0$=2 mol.L^{-1}, (b) 70 °C with CTA and $[AA]_0$=2 mol. L^{-1}, (c) 50 °C without CTA and $[AA]_0$=2 mol·L^{-1}, (d) 70 °C without CTA and $[AA]_0$=2 mol·L^{-1} . In all raw electropherograms, all PAA are injected at 2 different concentrations: the concentration at which no overloading occurs (see table S9) (blue line) and half of it (red line).

Dispersities of the distributions of electrophoretic mobilities

The dispersities of the distributions of electrophoretic mobilities, which are related to the heterogeneity of branching, are given by Eq. (S10) to (S13) [20]. They are all ratios of moments of different orders of the weight distribution of electrophoretic mobilities $W(\mu)$. Eq. (S14) gives the weight average electrophoretic mobility [20].

$$D(W(\mu),1,0) = \frac{[\sum_z W(\mu_z)\mu_z(\mu_{z+1}-\mu_z)][\sum_z W(\mu_z){\mu_z}^{-1}(\mu_{z+1}-\mu_z)]}{[\sum_z W(\mu_z)(\mu_{z+1}-\mu_z)]^2} \quad \text{(S10)}$$

$$D(W(\mu),2,0) = \frac{[\sum_z W(\mu_z){\mu_z}^2(\mu_{z+1}-\mu_z)]\,[\sum_z W(\mu_z)(\mu_{z+1}-\mu_z)]}{[\sum_z W(\mu_z)\mu_z(\mu_{z+1}-\mu_z)]^2} \quad \text{(S11)}$$

$$D(W(\mu),3,0) = \frac{[\sum_z W(\mu_z){\mu_z}^3(\mu_{z+1}-\mu_z)]\,[\sum_z W(\mu_z)\mu_z(\mu_{z+1}-\mu_z)]}{[\sum_z W(\mu_z){\mu_z}^2(\mu_{z+1}-\mu_z)]^2} \quad \text{(S12)}$$

$$D_\sigma = \left[\frac{[\sum_z W(\mu_z)(\mu_z-\mu_w)^2(\mu_{z+1}-\mu_z)]}{[\sum_z W(\mu_z)(\mu_{z+1}-\mu_z)]}\right]^{0.5} \quad \text{(S13)}$$

$$\mu_w = \frac{[\sum_z W(\mu_z)\mu_z(\mu_{z+1}-\mu_z)]}{[\sum_z W(\mu_z)(\mu_{z+1}-\mu_z)]} \quad \text{(S14)}$$

Table S13: Values of the dispersities and weight-average of the electrophoretic mobility distributions of PNaAs, with their average and standard deviation *SD*

Sample synthesis		$D(W(\mu),1,0)$	$D(W(\mu),2,0)$	$D(W(\mu),3,0)$	D_σ	μ_w ($m^2\ V^{-1}\ s^{-1}$)
50 °C without CTA and $[AA]_0$ = 2 M		1.00011	1.00011	1.00011	3.94×10^{-10}	3.76×10^{-8}
		1.00012	1.00012	1.00012	4.07×10^{-10}	3.72×10^{-8}
		1.00012	1.00012	1.00013	4.14×10^{-10}	3.73×10^{-8}
	average	1.000116667	1.000117	1.00012	4.05×10^{-10}	3.73515×10^{-8}
	SD	4.71405×10^{-6}	4.71×10^{-6}	8.16×10^{-6}	8.64×10^{-12}	1.6631×10^{-10}
70 °C without CTA and $[AA]_0$ = 2 M		1.00013	1.00013	1.00013	4.36×10^{-10}	3.77×10^{-8}
		1.00012	1.00012	1.00012	4.21×10^{-10}	3.79×10^{-8}
		1.00013	1.00013	1.00013	4.25×10^{-10}	3.75×10^{-8}
	average	1.000126667	1.000127	1.000127	4.27×10^{-10}	3.77×10^{-8}
	SD	4.71405×10^{-6}	4.71×10^{-6}	4.71×10^{-6}	6.07×10^{-12}	1.69056×10^{-10}
90 °C without CTA and $[AA]_0$ = 2 M		1.00013	1.00013	1.00013	4.30×10^{-10}	3.72×10^{-8}
		1.00012	1.00012	1.00012	4.05×10^{-10}	3.74×10^{-8}
		1.0001	1.0001	1.0001	3.82×10^{-10}	3.76×10^{-8}
	average	1.000116667	1.000117	1.000117	4.06×10^{-10}	3.74123×10^{-8}
	SD	1.24722×10^{-5}	1.25×10^{-5}	1.25×10^{-5}	1.96×10^{-11}	1.6696×10^{-10}
90 °C without CTA and $[AA]_0$ = 1 M		1.00014	1.00014	1.00014	4.43×10^{-10}	3.72×10^{-8}
		1.00012	1.00012	1.00012	4.07×10^{-10}	3.72×10^{-8}
		1.00011	1.00011	1.00011	3.95×10^{-10}	3.74×10^{-8}
	average	1.000123333	1.000123	1.000123	4.15×10^{-10}	3.72857×10^{-8}
	SD	1.24722×10^{-5}	1.25×10^{-5}	1.25×10^{-5}	2.02×10^{-11}	8.3467×10^{-11}
90 °C without CTA and $[AA]_0$ = 3 M		1.00012	1.00012	1.00012	4.16×10^{-10}	3.79×10^{-8}
		1.0001	1.0001	1.0001	3.81×10^{-10}	3.78×10^{-8}
		1.00012	1.00012	1.00012	4.22×10^{-10}	3.79×10^{-8}
	average	1.000113333	1.000113	1.000113	4.07×10^{-10}	3.78657×10^{-8}
	SD	9.42809×10^{-6}	9.43×10^{-6}	9.43×10^{-6}	1.79×10^{-11}	8.06687×10^{-11}
Linear PNaA [14]		1.00001	1.00001	1.00001	1.40×10^{-10}	3.86×10^{-8}
		1.00001	1.00001	1.00001	1.48×10^{-10}	3.86×10^{-8}
		1.00001	1.00001	1.00001	1.42×10^{-10}	3.88×10^{-8}
	average	1.00001	1.00001	1.00001	1.44×10^{-10}	3.86489×10^{-8}
	SD	0	0	0	3.43×10^{-12}	1.33498×10^{-10}

Reproducibility of the electrophoretic mobility distributions obtained from injections of PNaA at different pHs

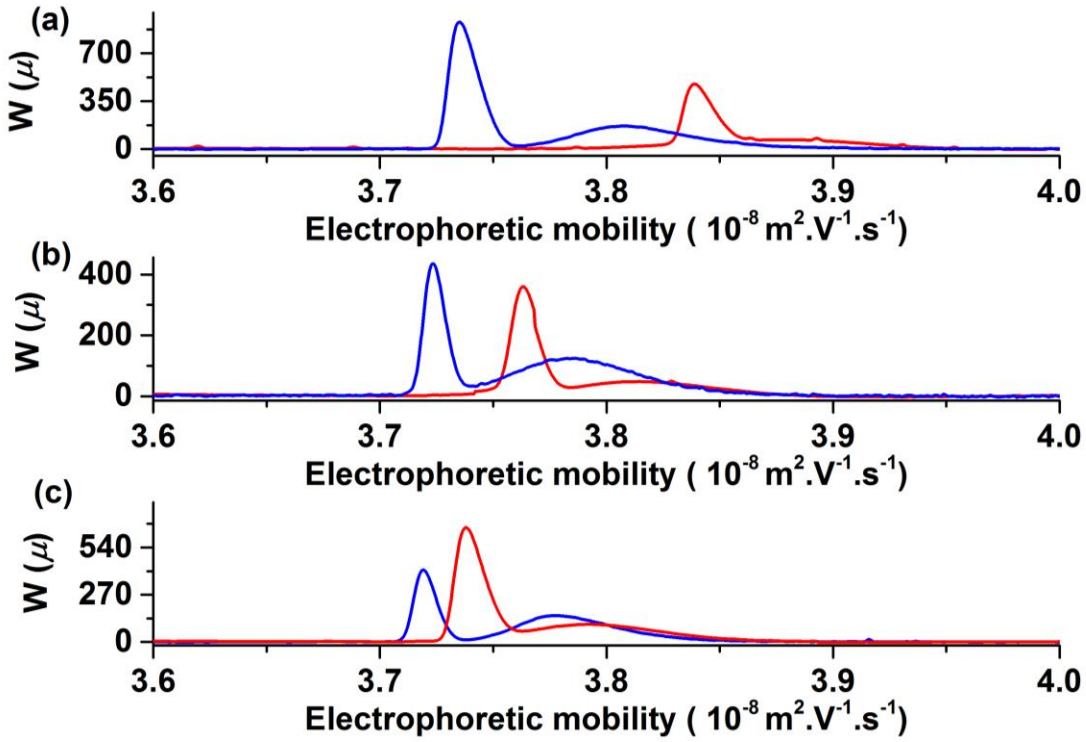

Figure S20: Electrophoretic mobility distributions of PNaA synthesized at 70 °C without CTA and $[AA]_0$=2 M (a), PNaA synthesized at 90 °C without CTA and $[AA]_0$=1 M (b), PNaA synthesized at 90 °C without CTA and $[AA]_0$=2 M (c). The PNaA were injected at pH between 4 and 5 (blue line) or between 8 and 9 (red line).

References

[1] M. Gaborieau, S.P.S. Koo, P. Castignolles, T. Junkers, C. Barner-Kowollik, Reducing the degree of branching in polyacrylates via midchain radical patching: A quantitative melt-state NMR study, Macromolecules 43 (2010) 5492-5495, 10.1021/ma100991c.

[2] D.C. Blackley, A.C. Haynes, Kinetics of thermal-decomposition of 4,4'-azobis-(4-cyanopentanoic acid) and its salts in aqueous-solution, J. Chem. Soc. Faraday Trans. I 75 (1979) 935-941, 10.1039/f19797500935.

[3] C. Loubat, B. Boutevin, Telomerization of acrylic acid with thioglycolic acid - Effect of the solvent on the C-T value, Polym. Bull. 44 (2000) 569-576, 10.1007/s002890070080.

[4] F.A. Plamper, H. Becker, M. Lanzendorfer, M. Patel, A. Wittemann, M. Ballauff, A.H.E. Muller, Synthesis, characterization and behavior in aqueous solution of star-shaped poly(acrylic acid), Macromol. Chem. Phys. 206 (2005) 1813-1825, 10.1002/macp.200500238.

[5] I. Lacik, S. Beuermann, M. Buback, PLP-SEC study into the free-radical propagation rate coefficients of partially and fully ionized acrylic acid in aqueous solution, Macromol. Chem. Phys. 205 (2004) 1080-1087,

[6] F.D. Kuchta, A.M. van Herk, A.L. German, Propagation kinetics of acrylic and methacrylic acid in water and organic solvents studied by pulsed-laser polymerization, Macromolecules 33 (2000) 3641-3649, 10.1021/ma990906t.

[7] H.L. Wang, H.R. Brown, Self-initiated photopolymerization and photografting of acrylic monomers, Macromol. Rapid Commun. 25 (2004) 1095-1099, 10.1002/marc.200400010.

[8] J. Barth, W. Meiser, M. Buback, SP-PLP-EPR study into termination and transfer kinetics of non-ionized acrylic acid polymerized in aqueous solution, Macromolecules 45 (2012) 1339-1345, 10.1021/ma202322a.

[9] S. Khanlari, M.A. Dube, Effect of pH on Poly(acrylic acid) Solution Polymerization, 52 (2015) 587-592, 10.1080/10601325.2015.1050628.

[10] J. Loiseau, N. Doerr, J.M. Suau, J.B. Egraz, M.F. Llauro, C. Ladaviere, Synthesis and characterization of poly(acrylic acid) produced by RAFT polymerization. Application as a very efficient dispersant of CaCO3, kaolin, and TiO2, Macromolecules 36 (2003) 3066-3077, 10.1021/ma0256744.

[11] J.-N. Ollagnier, T. Tassaing, S. Harrisson, M. Destarac, Application of online infrared spectroscopy to study the kinetics of precipitation polymerization of acrylic acid in supercritical carbon dioxide, 1 (2016) 372-378, 10.1039/C6RE00022C.

[12] N.F.G. Wittenberg, C. Preusser, H. Kattner, M. Stach, I. Lacík, R.A. Hutchinson, M. Buback, Modeling acrylic acid radical polymerization in aqueous solution, Macromol. React. Eng. 10 (2016) 95-107, 10.1002/mren.201500017.

[13] K.S. Anseth, R.A. Scott, N.A. Peppas, Effects of ionization on the reaction behavior and kinetics of acrylic acid polymerizations, Macromolecules 29 (1996) 8308-8312, 10.1021/ma960840r.

[14] A.R. Maniego, D. Ang, Y. Guillaneuf, C. Lefay, D. Gigmes, J.R. Aldrich-Wright, M. Gaborieau, P. Castignolles, Separation of poly(acrylic acid) salts according to topology using capillary electrophoresis in the critical conditions, Anal. Bioanal. Chem. 405 (2013) 9009-9020, 10.1007/s00216-013-7059-y.

[15] L. Couvreur, C. Lefay, J. Belleney, B. Charleux, O. Guerret, S. Magnet, First nitroxide-mediated controlled free-radical polymerization of acrylic acid, Macromolecules 36 (2003) 8260-8267, 10.1021/ma035043p.

[16] M.F. Llauro, J. Loiseau, F. Boisson, F. Delolme, C. Ladaviere, J. Claverie, Unexpected end-groups of poly(acrylic acid) prepared by RAFT polymerization, 42 (2004) 5439-5462, 10.1002/pola.20408.
[17] H.E. Gottlieb, V. Kotlyar, A. Nudelman, NMR chemical shifts of common laboratory solvents as trace impurities, J. Org. Chem. 62 (1997) 7512-7515, 10.1021/jo971176v.
[18] T.D.W. Claridge. High-resolution NMR techniques in organic chemistry, 2nd ed., Elsevier Science, Amsterdam, 2009.
[19] S. Schmitz, A.C. Dona, P. Castignolles, R.G. Gilbert, M. Gaborieau, Assessment of the extent of starch dissolution in dimethyl sulfoxide by 1H NMR spectroscopy, Macromol. Biosci. 9 (2009) 506-514, 10.1002/mabi.200800244.
[20] J.J. Thevarajah, A.T. Sutton, A.R. Maniego, E.G. Whitty, S. Harrisson, H. Cottet, P. Castignolles, M. Gaborieau, Quantifying the heterogeneity of chemical structures in complex charged polymers through the dispersity of their distributions of electrophoretic mobilities or of compositions, Anal. Chem. 88 (2016) 1674-1681, 10.1021/acs.analchem.5b03672.